

This is the author's peer reviewed, accepted manuscript. However, the online version of record will be different from this version once it has been copyedited and typeset.

PLEASE CITE THIS ARTICLE AS DOI: 10.1063/1.50045083

Assessment of Reynolds-averaged Navier–Stokes method for modeling the start-up regime of a Darrieus rotor

J.M. Ramírez* and Martín Saravia

Consejo Nacional de Investigaciones Científicas y Técnicas (CONICET),

Grupo de Investigación en Multifísica Aplicada (GIMAP),

Universidad Tecnológica Nacional FRBB (UTN),

11 de Abril 461, 8000 Bahía Blanca, Argentina

In this article, the suitability of the Reynolds-averaged Navier–Stokes (RANS) to predict the dynamic response in the startup process of small-scale Darrieus vertical-axis wind turbines (VAWT) was investigated. Using OpenFOAM, numerical simulations have been run to evaluate the regions of the rotor revolution where the prediction of the aerodynamic coefficients is expected to give unreliable results. The qualitative aspects of the prediction of the self-starting of the VAWT for tip speed ratio (λ) ranging from 0 to 3 have been evaluated and to model a more realistic condition, resistive forces acting on the rotor have been implemented. These resistive forces, which are the mechanical friction and the magnetic forces of the generator, were implemented numerically through a viscous damping model and, therefore, a new OpenFOAM library was developed adopting the object-oriented programming methodology as well as the C++ language. From the results, it has been observed that for a λ equal to 0.4 (starting speed), the aerodynamic forces are overestimated for a portion of 82% of the full revolution of the rotor. For a λ equal to 2.70 (steady state), this portion is reduced to 52%. This means that the aerodynamic forces and also the power output are overestimated by a large percentage in a full revolution of the rotor. Therefore, such results allow us to conjecture that RANS modeling may not seem to be an adequate approach to accurately assess the aerodynamic response of VAWTs.

* Corresponding author: jmramirez@bahiaablanca-conicet.gob.ar

I. INTRODUCTION

Nowadays, interest in sustainable electricity generation has grown due to the uncontrollable exploitation of non-renewable energy resources and their environmental pollution. For this reason, the use of renewable energy such as wind, solar and biomass has gained interest. Focusing on wind energy conversion devices, the vertical-axis wind turbine is a good candidate for urban applications. This device is mechanically simpler than the horizontal one since the vertical-axis wind turbine is able to provide a convincing performance even under unstable wind conditions without any need to be realigned. The fluid flow during the start and the stationary condition of the turbine could be characterized as unstable, therefore representing a considerable challenge to model the turbine by means of simulation tools.

Many researchers have used analytical models as the first method of calculation to study vertical-axis wind turbines (VAWTs). In this way, the design of an urban vertical-axis wind turbine and the prediction of its performance can be evaluated using (i) single stream tube models, (ii) multiple stream tube models, (iii) double multiple stream tube models, (iv) vortex models or, (v) cascade models [1–4]. The strength of these analytical models is their low computational cost, and their weakness is the prediction of aerodynamic forces when the turbine blades experience dynamic stall, a fact which is extremely relevant in self-starting conditions [5–7]. Therefore, computational fluid dynamics (CFD) has been the most adopted method to study urban VAWTs since it provides detailed information about the characteristics of the aerodynamic flow [8–20].

Currently, there are several articles in the scientific literature about CFD simulations of urban VAWTs whose models impose a constant rotation speed [21–24]. Franchina et al. [21] presented two-dimensional (2D) and three-dimensional (3D) numerical simulations of a Darrieus rotor using Ansys. The turbine was modeled with high and constant tip speed ratio (λ) values. From the results, a satisfactory correlation between numerical and experimental results was obtained. Wong et al. [22] studied the influence of a deflector plate located against the wind flow of the urban VAWT using NACA 0021 turbine blades. The simulation was performed using Ansys and it was validated by experiments carried out in a wind tunnel. The authors concluded that the turbine power coefficient had been significantly improved due to the implementation of the deflector plate. Marinić-Kragić et al. [23] investigated a novel design of VAWT with flexible blades. According to the authors, it could provide higher efficiency than conventional designs due to its capability to passively change shape on account of the aerodynamic forces generated by the fluid flow. The blades, optimized by using a genetic algorithm, rotated at a constant speed whilst the wind turbine was simulated using Ansys. Results showed the power coefficient of the optimized flexible blade had increased 8% in comparison with rigid blade designs although the flexible blade design presented limitations in

relation to structural damage. These authors have reported interesting numerical data about the performance of urban VAWTs. However, its self-starting was not modeled.

In order to model the self-start of urban VAWTs, the transient rotational speed must be considered in the numerical model. This speed is variable in time due to the forces generated on the blades by the fluid flow. For this purpose, the moment of inertia and the mechanical load on the rotor must be considered. Another primary aspect of modeling is the turbulence approach adopted to perform the simulations. This aspect is crucial to obtain an accurate prediction of aerodynamic forces. There are few published scientific articles treating the self-starting characteristics of urban VAWTs which include these fundamental aspects in their models [5–7]. Zhu et al. [5] studied the aerodynamic characteristics of the urban VAWT self-start with fluctuating wind speed using numerical simulations. From the results obtained, the authors observed a cyclical rotation during steady state and also an improvement of the self-starting aerodynamic characteristics. Zamani et al. [6] investigated a 3 kW VAWT using numerical simulations with OpenFOAM. The turbine blades were designed using a J-shaped profile. A SST $k - \omega$ turbulence model was used in the simulations. The numerical data obtained indicated an improved performance of the turbine self-start. Sun et al. [7] investigated the effects of using various aerodynamic profiles for the blades of an urban VAWT. For this purpose, the authors carried out numerical simulations in 2D and 3D utilizing the Spalart–Allmaras (SA) turbulence model. The authors concluded that the turbine performance was improved using an S-1046 aerodynamic profile for the blades instead of NACA 0018.

There are several models to solve the Navier–Stokes equations such as large eddy simulation (LES), detached eddy simulation (DES) and Reynolds-averaged Navier–Stokes (RANS). Due to its low computational cost, the RANS approach is commonly chosen for modeling urban VAWTs [25]. The precision of LES and DES certainly exceeds that of RANS, but their numerical requirements are often prohibitive. The RANS method uses various turbulence models to compute Reynolds stresses; single equation models as Spalart–Allmaras (SA), or two equation models, such as $k - \varepsilon$, $k - \omega$ or SST $k - \omega$ are commonly used [26]. The last one is a good option [27–31] because it is not overly sensitive to inlet boundary conditions and combines the advantages of the $k - \varepsilon$ and $k - \omega$ turbulence models in situations of adverse pressure gradients and boundary layer separations [26].

However, a known weakness of the RANS method is its inconsistency in predicting dynamic stall, which is particularly severe in urban VAWTs, and its occurrence is not only limited to machine start-up, but also to its operation. It is intuitive that errors in the prediction of the separation point could lead to the incorrect prediction of aerodynamic forces. Nevertheless, it is not clear how these errors are propagated when estimating the most important features of urban VAWTs: their power output and their ability to self-start. This point will be addressed in the next section. Therefore, an accurate prediction of aerodynamic forces is essential to determine the mechanical torque and

mechanical power of urban VAWTs. The turbulence approach to use is a crucial aspect to consider when modeling its self start performance.

The focus of this article is the suitability of RANS for predicting aerodynamic forces in this condition. The article is organized in the following manner. After the introduction, the design aspects of a low-power urban VAWT are presented in Section II. Section III presents the configuration of the numerical simulations. Section IV contains numerical results obtained from stationary flow simulations using NACA profiles 0012 and 0018. In addition, this section addresses discussions about the suitability of the RANS for predicting the dynamic response of small-scale VAWTs. Finally, section V presents the conclusions.

II. URBAN VAWTS

A. Design aspects

Urban VAWTs operate in an environment in which both the magnitude and direction of the wind are continuously changing. Although the change in wind direction does not affect the operation of the turbine, the change in magnitude certainly does. Small-scale turbines are typically light and must operate at high RPMs. Rotors have low inertia and they accelerate rapidly despite load control systems. These factors add complexity to the behavior of small-scale VAWTs which operate at a wide range of RPMs. From the simulation point of view, a reliable model should deliver results with reasonable accuracy for the whole range of operational speeds of the turbine. As stated before, RANS method can fail to predict separation of airfoil sections at large angles of attack (AoA) [32] and urban VAWTs can operate in this range. Assuming a constant direction and magnitude of the wind during a complete revolution of the rotor, a simple geometrical analysis would allow obtaining an analytical expression for the angle of attack α of the turbine blades as a function of their azimuthal position. Figure 1 shows the theoretical velocity triangle of a blade at an arbitrary azimuthal position.

Figure 1: Theoretical velocity triangle.

From the velocity triangle of a blade at an arbitrary angular position (see Fig. 1), the theoretical AoA for upwind ($0^\circ < \theta < 180^\circ$) and downwind ($180^\circ < \theta < 360^\circ$) is expressed as

$$\alpha = \tan^{-1} \left(\frac{\sin(\theta)}{\cos(\theta) + \lambda} \right) \quad (1)$$

where θ and λ are the azimuthal angle and the tip speed ratio, respectively. This expression is based on the assumption that the magnitude and direction of the wind velocity are fixed. Note that

θ is measured from the upper quadrant of the circle described by the rotor motion; in this case, blade #1 initial position coincides with this point.

The relative velocity w and the λ are defined as

$$w = U_{\infty} \sqrt{\lambda^2 + 2\lambda \cos(\theta) + 1} \quad (2)$$

$$\lambda = \frac{\omega R}{U_{\infty}} \quad (3)$$

being U_{∞} is the free stream velocity, R the rotor radius and ω is the rotor angular speed. Equation 1 clearly shows that AoA is dependent on both the environmental and geometrical parameters of the wind turbine.

The analysis will be focused on small-scale urban VAWTs of the Darrieus type, such as the one depicted in Fig. 2.

Figure 2: 3D design of a typical 3-blade urban VAWT.

These machines are typically designed using a set of parameters that are bounded between the limits presented in Table I [14]. The inlet speed is 10 m/s and it is calculated taking an average of the experimental measures at several urban locations.

Parameter	Value
Blades	3
Radius	[0.2, 0.4] m
Height	[0.5, 1.0] m
Blade chord length (c)	[0.05, 0.10] m
Blade section	NACA 0012, NACA 0018
Blade mounting point	$c/2$

Table I: Geometric parameters of an average urban VAWTs.

III. COMPUTATIONAL MODELING OF URBAN VAWTS IN OPENFOAM

Crucial aspects of the modeling process are the construction of the computational mesh and the configuration of the solver. In this section the typical decisions to be made for modeling in two dimensions urban VAWTs using RANS method are presented. The widely used SST $k-\omega$ turbulence approach is chosen [27–31].

A. Domain discretization

OpenFOAM uses the finite volume method for discretization of the domain. The discretization begins with the division of the VAWT computational domain in two circular regions, a rotating region comprising the rotor blades and a static region comprising the farfield.

Figure 3: Geometry scheme and boundary conditions of the urban VAWT.

In order to obtain accurate results, it is of primary importance to use a good quality computational grid; this implies both a strictly controlled density in specific areas and a smooth cell size transition between these areas and the free stream domain. For the case of VAWTs, a well-known meshing technique is the so-called O-mesh approach (see Fig. 4 and 5). This choice minimizes the skewness of near-wall cells, converging rapidly for high-order discretization schemes and also avoiding high aspect ratios.

(a)

(b)

Figure 4: (a) Overview of the computational mesh. (b) Close view of the static and dynamic mesh.

For an accurate determination of the aerodynamic forces over the blades, the boundary layer mesh is of utmost importance. Two approaches can be followed to capture the boundary layer dynamics, wall function modeling and resolution via inflation layer. The fact that the resolution of the boundary layer gives better results for aerodynamic coefficients is well documented [9, 33]. In this work, the boundary layer is resolved; so, the size near-wall cells have been defined so as to make the dimensionless wall distance $y^+ < 1$. Recall that y^+ is defined as $y^+ = \frac{u^* y}{\nu}$ where u^* is the friction velocity defined by $u^* = \sqrt{\frac{\tau_w}{\rho}}$, τ_w is the wall shear stress, y is the distance to the nearest wall and ν is the kinematic viscosity of the air. It is typically considered that the resolution of the boundary layer dynamics requires an inflation mesh with at least 20 sub-layers [20], and it is also a good practice to use an expansion ratio of 1.2 as well as a total layer thickness δ of 0.02 of the blade chord; Fig. 5 shows a blade meshed following this criterion (δ_1 is the thickness of the first sub-layer).

(a)(b)

Figure 5: (a) Close-up view of the grid at the leading and trailing edge. (b) Close-up view of BL mesh.

B. Solution

1. The OpenFOAM solver

The finite volume description of the rotor–flow interactions can be done through various formulations. Two of the most common are based on: non–moving volumes in a rotating frame of reference and moving volumes in an inertial frame of reference; in this paper, the latter one was chosen. OpenFOAM can effectively tackle the problem of transient flow interacting with moving solids through the `pimpleFoam` solver. `pimpleFoam` combines the PISO (Pressure-Implicit Split Operator) and SIMPLE (Semi Implicit Method for Pressure Linked Equations) solvers and is based on an Arbitrary Lagrangian–Eulerian (ALE) description, for which the mass and momentum balances are given by

$$\oint_{\partial\Omega} \mathbf{u} \cdot \hat{\mathbf{n}} dS = 0 \quad (4)$$

$$\int_{\Omega} \frac{\partial \mathbf{u}}{\partial t} d\Omega + \oint_{\partial\Omega} (\mathbf{F}_c - \mathbf{F}_s) dS = \int_{\Omega} \rho \mathbf{g} d\Omega \quad (5)$$

where \mathbf{u} is the fluid velocity, ρ is the fluid density, $\hat{\mathbf{n}}$ is the surface unit normal and \mathbf{g} is the gravity vector. The convective and stress forces are

$$\mathbf{F}_c = \rho \hat{\mathbf{n}} \cdot [\mathbf{u} \otimes (\mathbf{u} - \mathbf{u}_s)] \quad (6)$$

$$\mathbf{F}_s = \hat{\mathbf{n}} \cdot (-p\mathbf{I} + \boldsymbol{\tau}) \quad (7)$$

being \mathbf{u}_s the mesh velocity, p the pressure and $\boldsymbol{\tau}$ the viscous stress tensor.

For wind turbine applications it is possible to assume Newtonian incompressible flow so the stress tensor is

$$\boldsymbol{\tau} = \mu(\nabla \mathbf{u} + \nabla \mathbf{u}^T) \quad (8)$$

being μ the air viscosity.

The system of equations is closed with the relationship between the rate of change of the fluid cell volume and the mesh velocity \mathbf{u}_s ; this is, the integral space conservation law [34].

$$\frac{\partial}{\partial t} \int_{\Omega} d\Omega - \oint_{\partial\Omega} \mathbf{n} \cdot \mathbf{u}_s dS = 0 \quad (9)$$

2. Rotor dynamics

As mentioned previously, the domain is split into a moving inner zone and an outer static zone, which are in contact through an interface. Over this interface, fields are mapped; OpenFOAM automates the mapping process through the so-called arbitrary mesh interface boundary condition (AMI). Since the rotor flexibility is disregarded, the inner zone undergoes rigid body motion. Under this assumption, the rate of change of the cell volume is zero, and therefore Eq. 9 is no longer required.

The velocity \mathbf{u}_s in Eq. 6 is the result of its rigid rotation around the rotor axis; so, the mesh position is obtained by numerically integrating a set of 6 second order ODEs and then recalling the kinematic relation

$$\mathbf{u}_s = \dot{\mathbf{x}}_0 + \dot{\mathbf{\Lambda}} \mathbf{r} \quad (10)$$

where \mathbf{x}_0 is the center of rotation, $\mathbf{\Lambda}$ is the rotation tensor and \mathbf{r} is the relative position of a point in the mesh with respect to the center of rotation. Note that the dot has been used to represent time derivatives.

OpenFOAM can solve the rotor motion via a six degree of freedom model that parametrizes finite rotations with quaternions; the model is implemented in the library "`sixDoFRigidBodyMotion`". However, this model does not include the effect of resistive forces; so, for this paper, an algorithm that can take into account resistive forces was developed and implemented in a new library.

3. Resistive forces modeling

The rotor transient dynamic is governed by the interaction between aerodynamic and internal electro-mechanical forces; the latter are resistive in nature. The most important electro-mechanical forces are originated by mechanical friction and electromagnetic induction. In order to study the transient behavior of the rotor, a new OpenFOAM library implementing these effects has been developed. This new library is based on the existing "`sixDoFRigidBodyMotion`" library; so all existing time integration algorithms can be used. For the simulations presented in the next sections,

the Newmark integrator was chosen.

A key advantage of the adopted approach is that it allows the execution of inner iteration loops between the rigid body solver and the fluid solver in order to guarantee the convergence of the electro-mechanical and aerodynamic torques.

The resistive forces are considered with a viscous damping model in which the magneto-mechanical torque is assumed to be proportional to the angular position and velocity of the rotor and they are condensed in a single coefficient c_R . So, the total resistive torque is calculated as

$$T = c_R(\theta, \omega) \omega \quad (11)$$

where θ is the angular position of the rotor and ω the rotational speed of the wind turbine. The functionality with θ arises from the magnet-coil interaction in the electric generator, while the functionality with ω arises from viscous friction in the mechanical components.

IV. NUMERICAL TESTS

A. Static airfoils in steady flow

In this section the suitability of the SST $k-\omega$ turbulence model for the prediction of aerodynamic coefficients of airfoil sections in steady flow is addressed. Two of the most commonly used profiles in urban vertical-axis wind turbines, namely the NACA 0012 and 0018, have been tested. In order to determine the angle of attack values of the blades as a function of the azimuthal angle of the rotor, Eq. 1 has been used setting the rotor radius as 0.3 m and the free stream velocity as 10 m/s. Figure 6 shows the variation of the AoA over the azimuthal angle of the rotor ranging from 0° to 180° .

Figure 6: Blade angle of attack as a function of the azimuthal angle and λ of the rotor.

After observing the curves in Fig. 6, it can be appreciated that the blades present large AoA values in a large portion of the rotor revolution. One of the key aspects of the design of VAWTs is the estimation of its power output, which is controlled by the aerodynamic forces acting on the blades. Since these forces can be reasonably determined by the aerodynamic coefficients, it is assumed they can be taken as the key parameters that determine the suitability of SST $k-\omega$ turbulence model for the problem in question. For making an assessment of the capability of the model, the aerodynamic coefficients have been numerically obtained in steady flow for NACA 0012 and 0018 airfoils. These simulations are compared with experiments [35] for AoA values ranging from 0° to 180° . The Reynolds number is 7.7×10^4 . Note that this Reynolds number is a mean value of the urban VAWT operational

regime for typical geometric parameters (see Table I). The aerodynamic coefficients in steady flow for NACA 0012 and 0018 airfoils can be appreciated in Figs. 7 and 8.

(a)

Figure 7: Airfoil NACA 0012. (a) Drag and (b) Lift coefficients as a function of the angle of attack.

(b)

Figure 8: Airfoil NACA 0018. (a) Drag and (b) Lift coefficients as a function of the angle of attack.

From Figs. 7 and 8, it can be observed that both drag and lift coefficients are accurately captured by the numerical model at values of AoA $\pm 15^\circ$ of 0° and 180° . However, aerodynamic forces for angles higher than 15° are not in concordance compared with experiments [35]. It is important to notice that the experimental values of NACA 0012 airfoil for both drag and lift coefficients for values of AoA of 5° , 10° and 15° , illustrated in Figs. 7 and 8, are taken into account from [36] due to the fact that there are no consistent values for these cases in [35].

B. Aerodynamic coefficients of our urban VAWT

In this section, an assessment is made of the potential impact of the inaccuracies in the determination the aerodynamic coefficients presented in the last section. These inaccuracies have an important role in the estimation of the power output and the self-starting capabilities of urban VAWTs. For this purpose, numerical simulations have been executed to determine the portion in a complete rotor revolution in which the blades present AoA values higher than 15° , which is the limit for which the SST $k - \omega$ gives an average error of 5%. It is of importance the fact that, although possible, this evaluation was not performed using the results presented in Fig. 6, because blade interaction is supposed to play an important role in the determination of aerodynamics forces. With this evaluation, it is possible to judge the suitability of the SST $k - \omega$ turbulence approach for the prediction of the self-start of urban turbines.

For this test case, the numerical simulations have been carried out using a free-stream velocity of $10 \frac{m}{s}$ and a NACA 0012 airfoil profile. Figure 9 shows the drag coefficient as a function of the azimuthal angle for various λ values. Figure 10 shows the moment coefficient as a function of the azimuthal angle.

(a)

(b)

Figure 9: Drag coefficient as a function of azimuthal angle. For a λ equal to (a) 0.40, (b) 1.05, (c) 2.10 and, (d) 2.70.

(c)

(d)

Figure 10: Moment coefficient as a function of azimuthal angle. For a λ equal to (a) 0.40, (b) 1.05, (c) 2.10 and, (d) 2.70.

As the figure illustrates, at λ equal to 0.40 (14 rad/s), 82% of the complete rotor revolution presents AoAs higher than 15° . At λ equal to 1.05 (35 rad/s), the blade presents AoA higher than 15° for a portion of 82% of the complete rotor revolution. For λ equal to 2.10 (70 rad/s), this portion is decreased to 64%. When the turbine is accelerated it reaches λ equal to 2.70 (90 rad/s), the area with large AoA values is decreased, reaching 52%.

The moment coefficient is an important parameter to evaluate the performance of an urban VAWT. This parameter is dimensionless and can have positive or negative sign. A positive value of the moment coefficient represents that the rotor is rotating and as consequence the turbine has energy available to be transformed by the electric motor. The movement of rotation occurs when the forces generated on the blades by the fluid flow overcome the friction forces of the rotor and those generated by the electric motor. A negative value of this coefficient represents a deceleration of the rotor. The power available has been estimated numerically integrating the moment coefficient curves depicted in Fig. 10. The power coefficient is defined as the scalar product between the moment coefficient and the rotation speed [1]. Hence, the percentage of the power available which corresponds to the region that the blades present AoA values $\pm 15^\circ$ of 0° and 180° has been determined; i.e. in areas for which the aerodynamic forces obtained from the numerical simulation are over-estimated. In Table 3, the percentage of the power available has been presented in a complete rotor revolution for various λ values.

λ	% of power available
	$\alpha > 15^\circ $
0.40	94.0
1.05	93.4
2.10	91.4
2.70	71.3

Table II: Percentage of power available vs. λ values for AoA values higher than $\pm 15^\circ$ of 0° and 180° .

From the results obtained in Table 3, it is observed that the percentage of the power available for AoA values higher than 15° decreases as λ values increase. In the turbine start-up condition, for a λ equal to 0.4, the percentage of the power available is 94% in a complete rotor revolution. In the stationary condition, for a λ equal to 2.70, the power available is 71%. This means that the aerodynamic forces are overestimated for a large percentage of the power available in a complete rotor revolution. Therefore, the power output is also overestimated.

C. Impact on the working condition

The above results raise a question about the impact of a bad prediction in the aerodynamic coefficients in the working condition of the wind turbine. In order to partially answer it, we simulate the starting-to-regime response of a typical turbine for different load conditions. Figure 11 shows the corresponding time history of the λ and mechanical power generated by the rotor for different mechanical loads.

(a)

Figure 11: Time response of the urban turbine for various mechanical loads (c_R) (Nms/rad). (a) tip speed ratio vs. time and (b) mechanical power vs. time.

From the results exhibited in Fig. 11 it can be confirmed the expected behavior, the wind turbine reaches a maximum rotational speed that is a function of both: the resistive mechanical torque acting on the rotor and its inertia. The figure shows that for the present rotor, the zero load case gives a maximum rotational speed corresponding to a λ of approximately 3. Taking into account the results of section IV-B, it can be seen that this case corresponds to the most favorable situation, since the part of the rotor revolution in which the blade is working with an angle of attack less than 15% is the highest. However, considering the results obtained in section IV-A it can be observed that for

this value of λ , the angle of attack of the blades changes between 0° and 20° for the rotor revolution, which suggests that still in this highly favorable case, the aerodynamic forces in a 44% portion of the rotor revolution are overestimated, which suggests that not only the time to reach the stationary condition but also the final rotational speed of the no-load case are not correctly predicted.

When power is taken out from the rotor, the rotational velocity decreases, the case of maximum power output corresponds to a c_R coefficient of 0.03, and a λ of 1.8. The results of section IV-B suggest that the situation is worse than for the zero mechanical load; in fact, from Table II it can be seen that 90% of the power output was generated at angles of attack for which the RANS solution over predicts the aerodynamic forces up to a factor of 1.7. The same conclusion can be drawn for all rotational speeds and all mechanical load coefficients.

V. CONCLUSION

The suitability of RANS modeling for the estimation of the dynamic response of small-scale VAWT has been investigated. The aerodynamic coefficients for a wide range of angles of attack has been obtained for two of the most common airfoil profiles used in this application, namely the NACA 0012 and NACA 0018. The numerical results were compared with experimental data in order to identify the region of the coefficient vs. angle curve where the numerical model gave an incorrect prediction; results suggest that the RANS prediction is acceptable for angles of attack smaller than 15%. After identifying this threshold value, several working scenarios of a common small-scale wind turbine configuration were simulated and the percentage of the power output that was estimated above and below the threshold was quantified. Results allow concluding that RANS modeling may not be adequate to assess the dynamics of small-scale wind turbines. In light of these conclusions, improvement of existing RANS capabilities, such as incorporating evolutionary and genetic algorithms to calibrate the turbulence coefficients, or developing new models, appears to be necessary to obtain an accurate prediction of the power output of urban VAWTs.

ACKNOWLEDGMENTS

This work was supported by the Consejo Nacional de Investigaciones Científicas y Técnicas (CONICET) and Universidad Tecnológica Nacional. In addition, the authors would like to thank Prof. Madeleine Raño for correcting the English language of the manuscript.

DATA AVAILABILITY

The data that support the findings of this study are available within the article.

-
- [1] I. Paraschivoiu, Wind Turbine Design, presses in Edition, Polytechnic international Press, Canada, 2002 (2002).
 - [2] M. Abdul Akbar, V. Mustafa, A new approach for optimization of Vertical Axis Wind Turbines, Journal of Wind Engineering and Industrial Aerodynamics 153 (2016) 34–45 (2016). doi:10.1016/j.jweia.2016.03.006.
 - [3] Z. Zhao, C. Yan, T. Wang, B. Xu, Y. Zheng, Study on approach of performance improvement of VAWT employing double multiple stream tubes model, Journal of Renewable and Sustainable Energy 9 (2) (2017). doi:10.1063/1.4979356.
 - [4] Z. Zhao, D. Su, T. Wang, B. Xu, H. Wu, Y. Zheng, A blade pitching approach for vertical axis wind turbines based on the free vortex method, Journal of Renewable and Sustainable Energy 11 (5) (2019). doi:10.1063/1.5099411.
 - [5] Effect of wind fluctuating on self-starting aerodynamics characteristics of VAWT, Journal of Central South University 23 (8) (2016) 2075–2082 (2016). doi:10.1007/s11771-016-3263-1.
 - [6] M. Zamani, M. J. Maghrebi, S. R. Varedi, Starting torque improvement using J-shaped straight-bladed Darrieus vertical axis wind turbine by means of numerical simulation, Renewable Energy 95 (2016) 109–126 (2016). doi:10.1016/j.renene.2016.03.069.
 - [7] X. Sun, J. Zhu, A. Hanif, Z. Li, G. Sun, Effects of blade shape and its corresponding moment of inertia on self-starting and power extraction performance of the novel bowl-shaped floating straight-bladed vertical axis wind turbine, Sustainable Energy Technologies and Assessments 38 (December 2019) (2020) 100648 (2020). doi:10.1016/j.seta.2020.100648.
 - [8] A. R. Sengupta, A. Biswas, R. Gupta, The aerodynamics of high solidity unsymmetrical and symmetrical blade H-Darrieus rotors in low wind speed conditions, Journal of Renewable and Sustainable Energy 9 (4) (2017). doi:10.1063/1.4999965.
 - [9] M. Ghasemian, Z. N. Ashrafi, A. Sedaghat, A review on computational fluid dynamic simulation techniques for Darrieus vertical axis wind turbines, Energy Conversion and Management 149 (2017) 87–100 (2017). doi:10.1016/j.enconman.2017.07.016.
 - [10] G. Bangga, T. Lutz, A. Dessoky, E. Krämer, Unsteady Navier-Stokes studies on loads, wake, and dynamic stall characteristics of a two-bladed vertical axis wind turbine, Journal of Renewable and Sustainable Energy 9 (5) (2017). arXiv:1708.08365, doi:10.1063/1.5003772.

This is the author's peer reviewed, accepted manuscript. However, the online version of record will be different from this version once it has been copyedited and typeset.

PLEASE CITE THIS ARTICLE AS DOI: 10.1063/1.50045083

- [11] H. Sundararaju, K. H. Lo, R. Metcalfe, S. S. Wang, Aerodynamics and CFD analysis of equal size dual-rotor wind turbine, *Journal of Renewable and Sustainable Energy* 9 (4) (2017). doi:10.1063/1.4999500.
- [12] J. Chen, P. Liu, H. Xu, L. Chen, M. Yang, L. Yang, A detailed investigation of a novel vertical axis Darrieus wind rotor with two sets of blades, *Journal of Renewable and Sustainable Energy* 9 (1) (2017). doi:10.1063/1.4977004.
- [13] F. Toja-Silva, T. Kono, C. Peralta, O. Lopez-Garcia, J. Chen, A review of computational fluid dynamics (CFD) simulations of the wind flow around buildings for urban wind energy exploitation, *Journal of Wind Engineering and Industrial Aerodynamics* 180 (July) (2018) 66–87 (2018). doi:10.1016/j.jweia.2018.07.010.
- [14] A. Rezaeiha, H. Montazeri, B. Blocken, Towards optimal aerodynamic design of vertical axis wind turbines: Impact of solidity and number of blades, *Energy* 165 (2018) 1129–1148 (2018). doi:10.1016/j.energy.2018.09.192.
URL <https://doi.org/10.1016/j.energy.2018.09.192>
- [15] H. F. Lam, Y. M. Liu, H. Y. Peng, C. F. Lee, H. J. Liu, Assessment of solidity effect on the power performance of H-rotor vertical axis wind turbines in turbulent flows, *Journal of Renewable and Sustainable Energy* 10 (2) (2018). doi:10.1063/1.5023120.
- [16] P. Benard, A. Viré, V. Moureau, G. Lartigue, L. Beaudet, P. Deglaire, L. Bricteux, Large-Eddy Simulation of wind turbines wakes including geometrical effects, *Computers and Fluids* 173 (2018) 133–139 (2018). doi:10.1016/j.compfluid.2018.03.015.
- [17] K. Asada, S. Kawai, Large eddy simulation of airfoil flow near stall condition at Reynolds number 2.1e6, *Physics of Fluids* 30 (8) (2018). doi:10.1063/1.5037278.
- [18] B. Mannion, S. B. Leen, S. Nash, A two and three-dimensional CFD investigation into performance prediction and wake characterisation of a vertical axis turbine, *Journal of Renewable and Sustainable Energy* 10 (3) (2018). doi:10.1063/1.5017827.
- [19] H. Y. Peng, H. F. Lam, H. J. Liu, Numerical investigation into the blade and wake aerodynamics of an H-rotor vertical axis wind turbine, *Journal of Renewable and Sustainable Energy* 10 (5) (2018). doi:10.1063/1.5040297.
- [20] G. Bangga, A. Dessoky, Z. Wu, K. Rogowski, M. O. Hansen, Accuracy and consistency of CFD and engineering models for simulating vertical axis wind turbine loads, *Energy* 206 (2020) 118087 (2020). doi:10.1016/j.energy.2020.118087.
- [21] N. Franchina, G. Persico, M. Savini, 2D-3D Computations of a Vertical Axis Wind Turbine Flow Field: Modeling Issues and Physical Interpretations, *Renewable Energy* 136 (2019) 1170–1189 (2019). doi:10.1016/j.renene.2018.09.086.

- [22] K. H. Wong, W. T. Chong, S. C. Poh, Y. C. Shiah, N. L. Sukiman, C. T. Wang, 3D CFD simulation and parametric study of a flat plate deflector for vertical axis wind turbine, *Renewable Energy* 129 (2018) 32–55 (2018). doi:10.1016/j.renene.2018.05.085.
- [23] I. Marinić-Kragić, D. Vučina, Z. Milas, Concept of flexible vertical-axis wind turbine with numerical simulation and shape optimization, *Energy* 167 (2019) 841–852 (2019). doi:10.1016/j.energy.2018.11.026.
- [24] L. Zhang, K. Zhu, T. Jiang, L. Zhang, S. Li, X. Zhao, Numerical investigations of the effect of rotating and non-rotating shaft on aerodynamic performance of small scale urban vertical axis wind turbines, *Journal of Renewable and Sustainable Energy* 10 (4) (2018). doi:10.1063/1.5025078.
- [25] H. Yu, J. Thé, Validation and optimization of SST $k-\omega$ turbulence model for pollutant dispersion within a building array, *Atmospheric Environment* 145 (2016) 225–238 (2016). doi:10.1016/j.atmosenv.2016.09.043.
- [26] F. Moukalled, L. Mangani, M. Darwish, *The Finite Volume Method in Computational Fluid Dynamics*, Vol. 113, 2016 (2016). arXiv:arXiv:1011.1669v3, doi:10.1007/978-3-319-16874-6.
- [27] M. W. Lohry, L. Martinelli, Unsteady reynolds-averaged navier-stokes simulation of crossflow rotors, scaling, and blockage effects, *AIAA Journal* 54 (12) (2016) 3828–3839 (2016). doi:10.2514/1.J055069.
- [28] M. M. Bhargav, V. Ratna Kishore, V. Laxman, Influence of fluctuating wind conditions on vertical axis wind turbine using a three dimensional CFD model, *Journal of Wind Engineering and Industrial Aerodynamics* 158 (April) (2016) 98–108 (2016). doi:10.1016/j.jweia.2016.10.001.
- [29] A. Rezaeiha, I. Kalkman, B. Blocken, Effect of pitch angle on power performance and aerodynamics of a vertical axis wind turbine, *Applied Energy* 197 (2017) 132–150 (2017). doi:10.1016/j.apenergy.2017.03.128.
- [30] F. Balduzzi, J. Drofelnik, A. Bianchini, G. Ferrara, L. Ferrari, M. S. Campobasso, Darrieus wind turbine blade unsteady aerodynamics: a three-dimensional Navier-Stokes CFD assessment, *Energy* 128 (2017) 550–563 (2017). doi:10.1016/j.energy.2017.04.017.
- [31] S. Zanforlin, S. Deluca, Effects of the Reynolds number and the tip losses on the optimal aspect ratio of straight-bladed Vertical Axis Wind Turbines, *Energy* 148 (2018) 179–195 (2018). doi:10.1016/j.energy.2018.01.132.
URL <https://doi.org/10.1016/j.energy.2018.01.132>
- [32] H. Y. Xu, C. L. Qiao, H. Q. Yang, Z. Y. Ye, Delayed detached eddy simulation of the wind turbine airfoil S809 for angles of attack up to 90 degrees, *Energy* 118 (2017) 1090–1109 (2017). doi:10.1016/j.energy.2016.10.131.
- [33] F. Balduzzi, A. Bianchini, G. Ferrara, L. Ferrari, Dimensionless numbers for the assessment of mesh and timestep requirements in CFD simulations of Darrieus wind turbines, *Energy* 97 (2016) 246–261

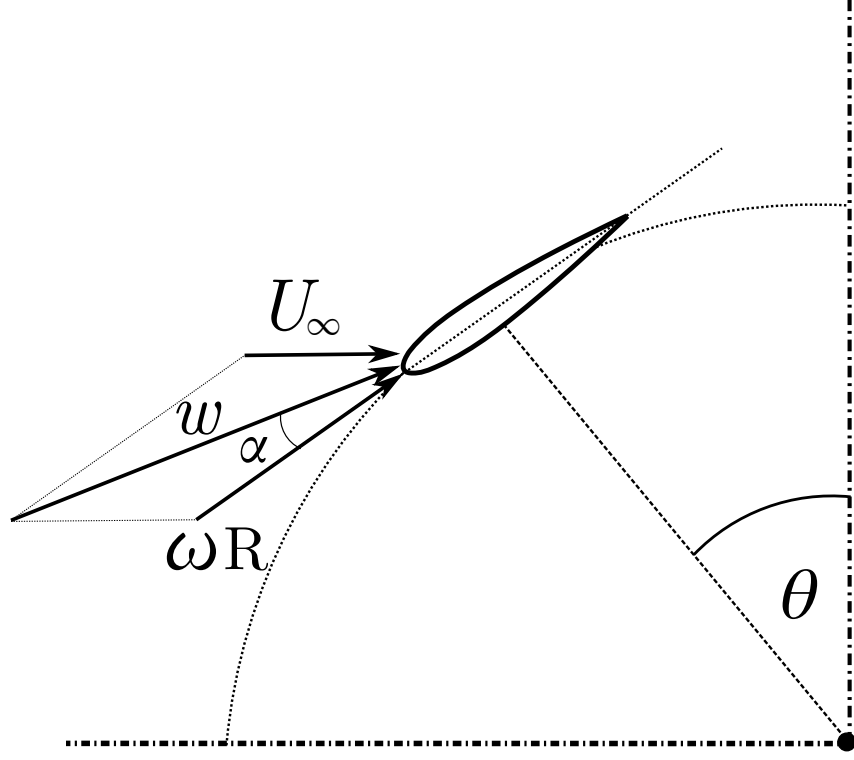
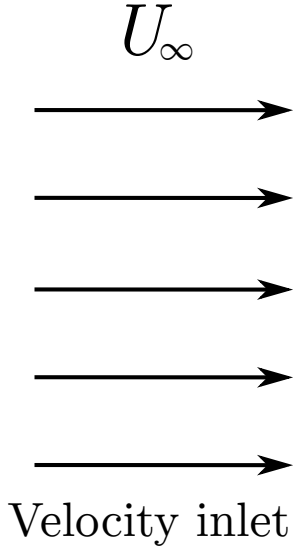
This is the author's peer reviewed, accepted manuscript. However, the online version of record will be different from this version once it has been copyedited and typeset.

PLEASE CITE THIS ARTICLE AS DOI: 10.1063/1.50045083

- (2016). doi:10.1016/j.energy.2015.12.111.
- [34] I. Demirdzic, M. Peric, Space conservation law in finite volume calculations of fluid flow., *International journal for numerical methods in fluids* 8 (9) (1988) 1037–1050 (1988).
- [35] R. E. Sheldahl, P. C. Klimas, Aerodynamic characteristics of seven symmetrical airfoil sections through 180-degree angle of attack for use in aerodynamic analysis of vertical axis wind turbines., *Tech. rep.*, Sandia National Laboratories, Albuquerque, NM (USA) (1981).
- [36] Z. Li, L. Feng, H. R. Karbasian, J. Wang, K. C. Kim, Experimental and numerical investigation of three-dimensional vortex structures of a pitching airfoil at a transitional Reynolds number, *Chinese Journal of Aeronautics* 32 (10) (2019) 2254–2266 (2019). doi:10.1016/j.cja.2019.04.015.

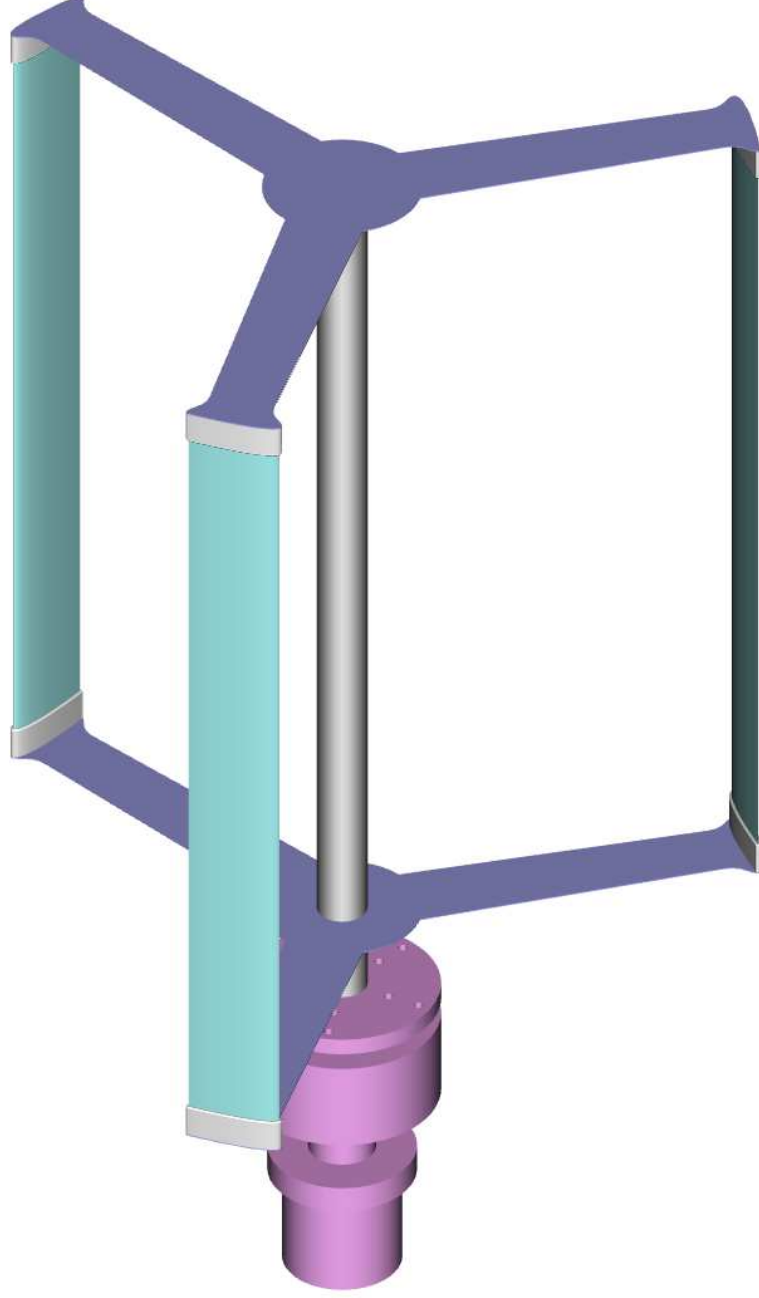
This is the author's peer reviewed, accepted manuscript. However, the online version of record will be different from this version once it has been copyedited and typeset.

PLEASE CITE THIS ARTICLE AS DOI: 10.1063/5.0045083



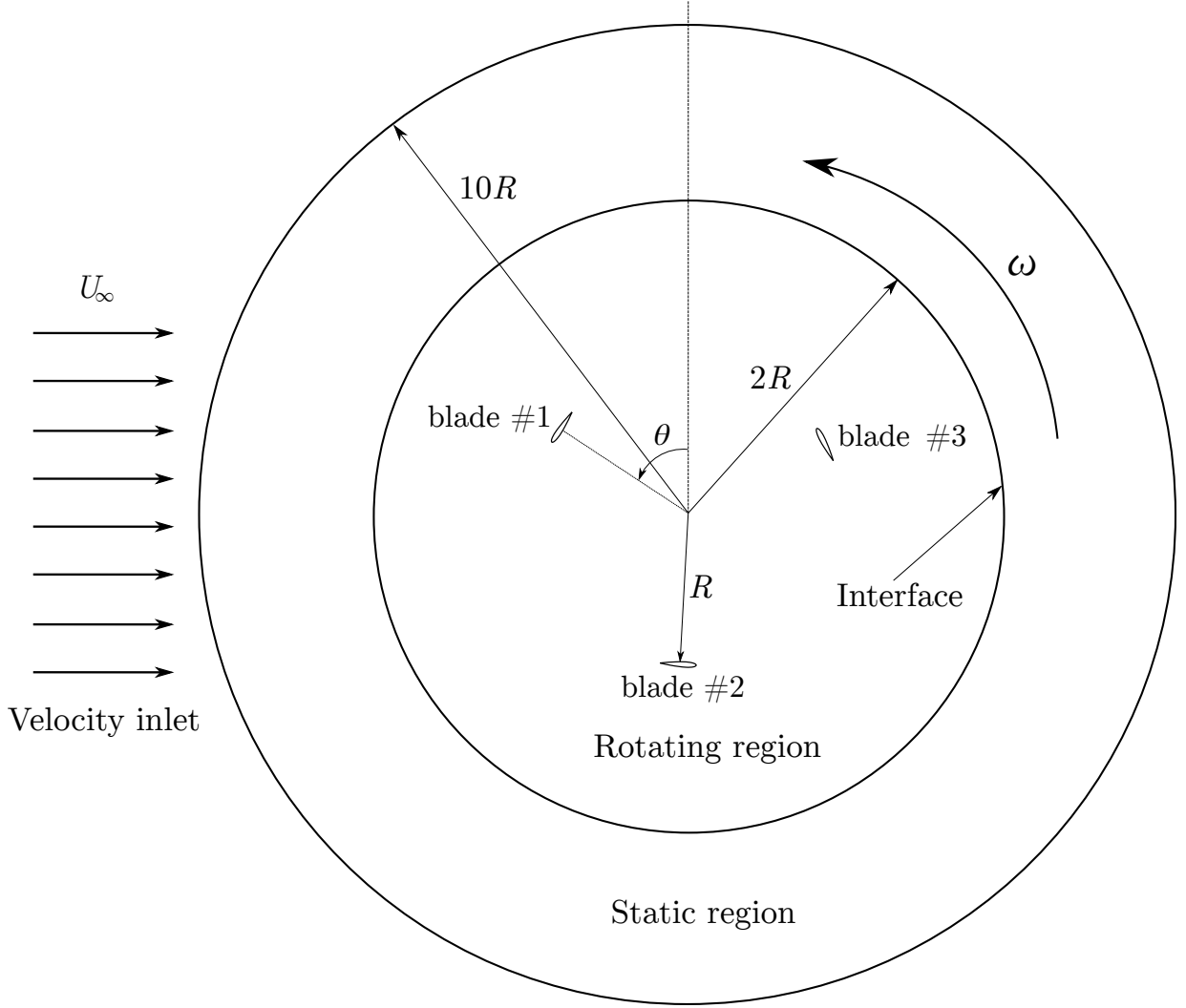
This is the author's peer reviewed, accepted manuscript. However, the online version of record will be different from this version once it has been copyedited and typeset.

PLEASE CITE THIS ARTICLE AS DOI: 10.1063/1.50045083



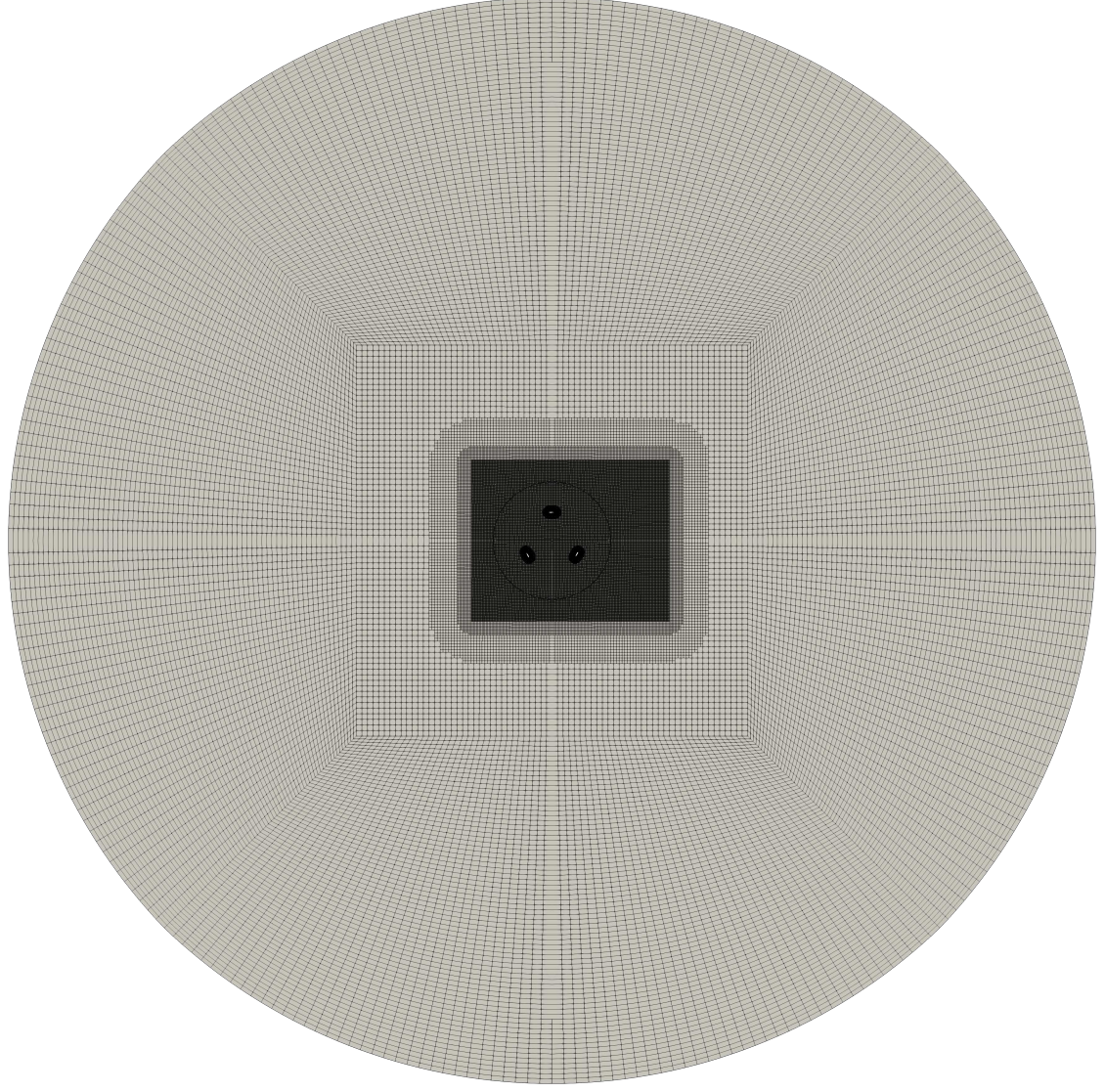
This is the author's peer reviewed, accepted manuscript. However, the online version of record will be different from this version once it has been copyedited and typeset.

PLEASE CITE THIS ARTICLE AS DOI: 10.1063/5.0045083



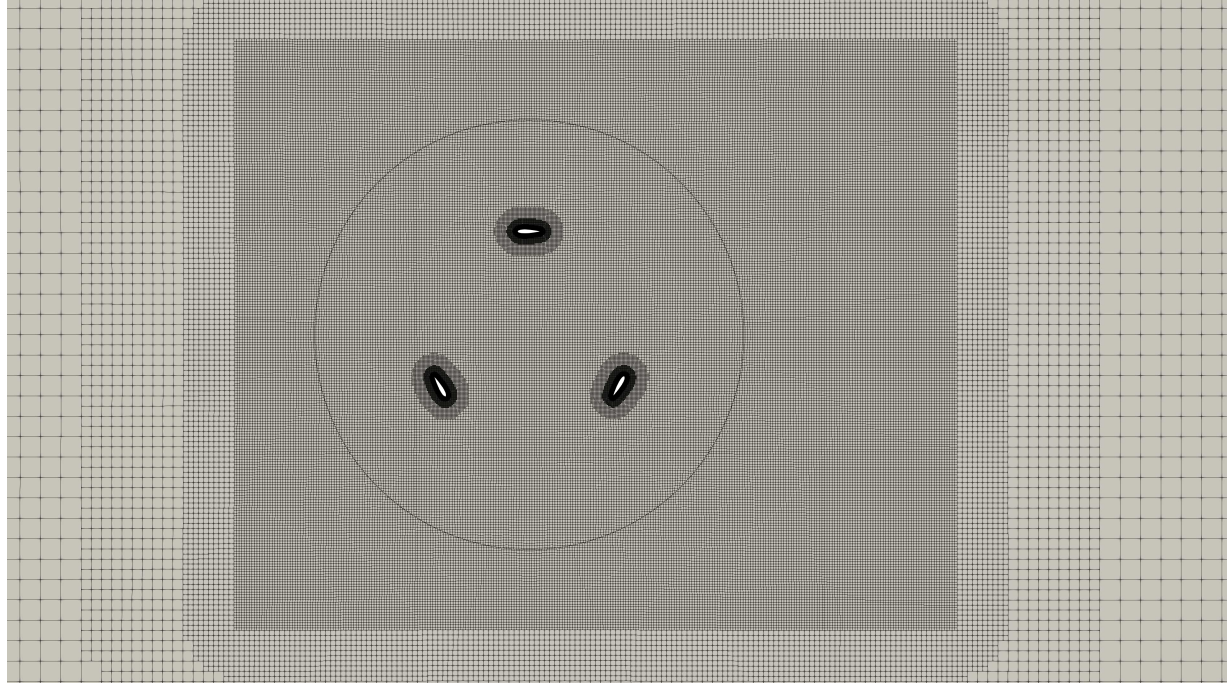
This is the author's peer reviewed, accepted manuscript. However, the online version of record will be different from this version once it has been copyedited and typeset.

PLEASE CITE THIS ARTICLE AS DOI: 10.1063/1.50045083



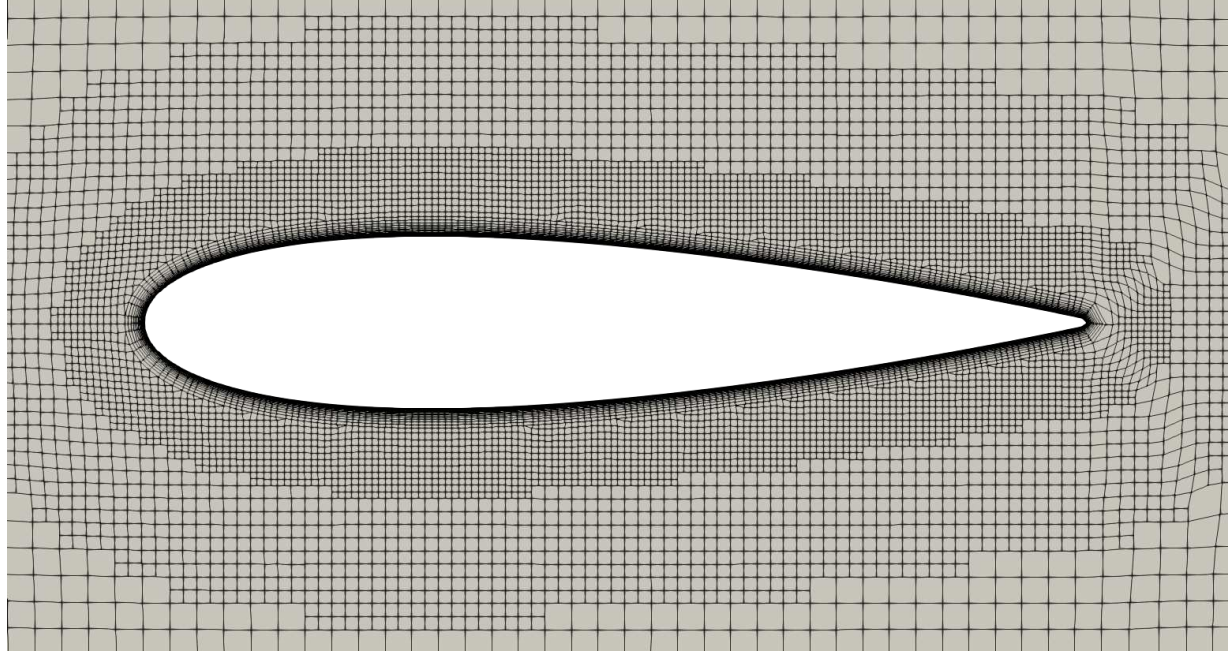
This is the author's peer reviewed, accepted manuscript. However, the online version of record will be different from this version once it has been copyedited and typeset.

PLEASE CITE THIS ARTICLE AS DOI: 10.1063/1.50045083



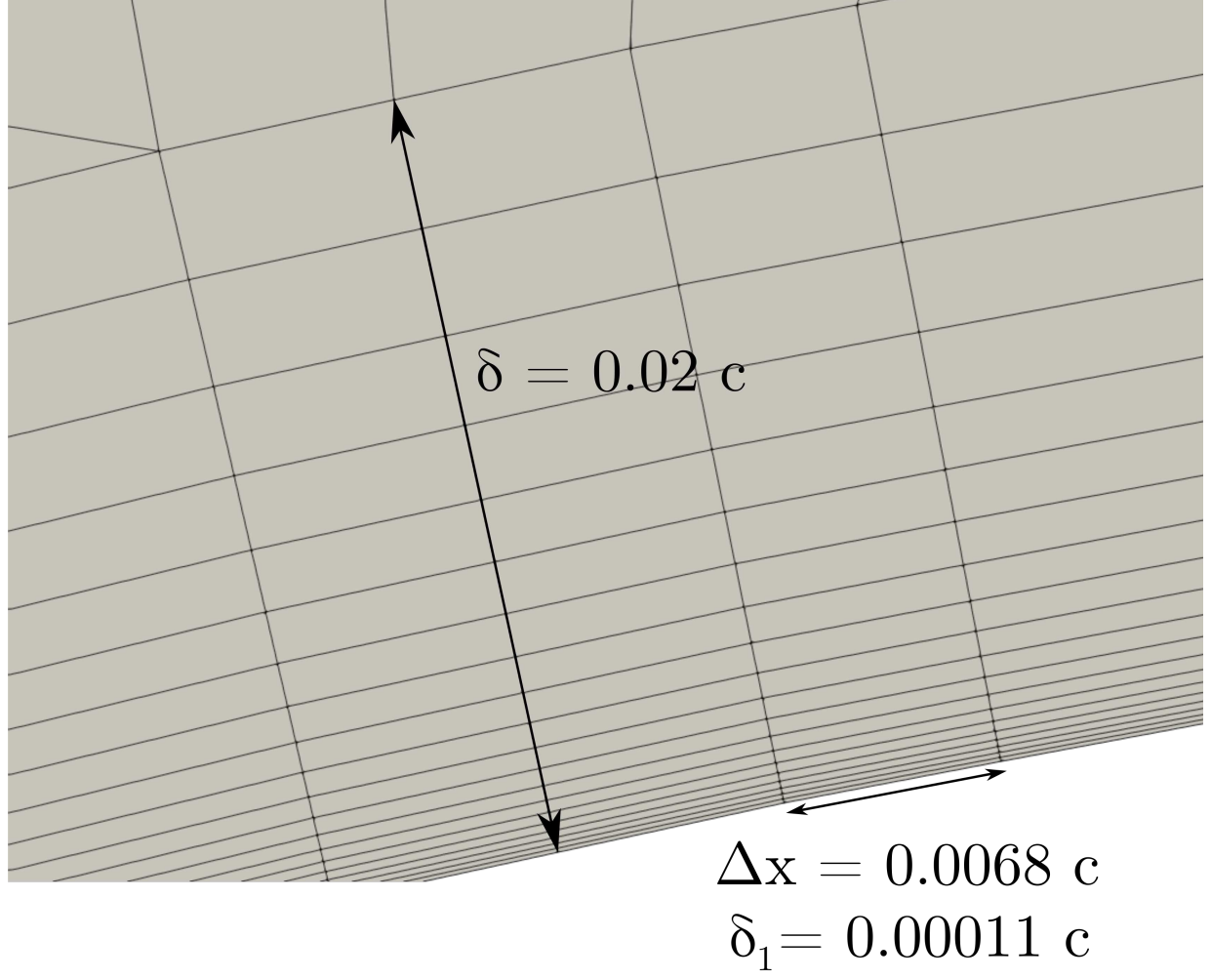
This is the author's peer reviewed, accepted manuscript. However, the online version of record will be different from this version once it has been copyedited and typeset.

PLEASE CITE THIS ARTICLE AS DOI: [10.1063/5.0045083](https://doi.org/10.1063/5.0045083)



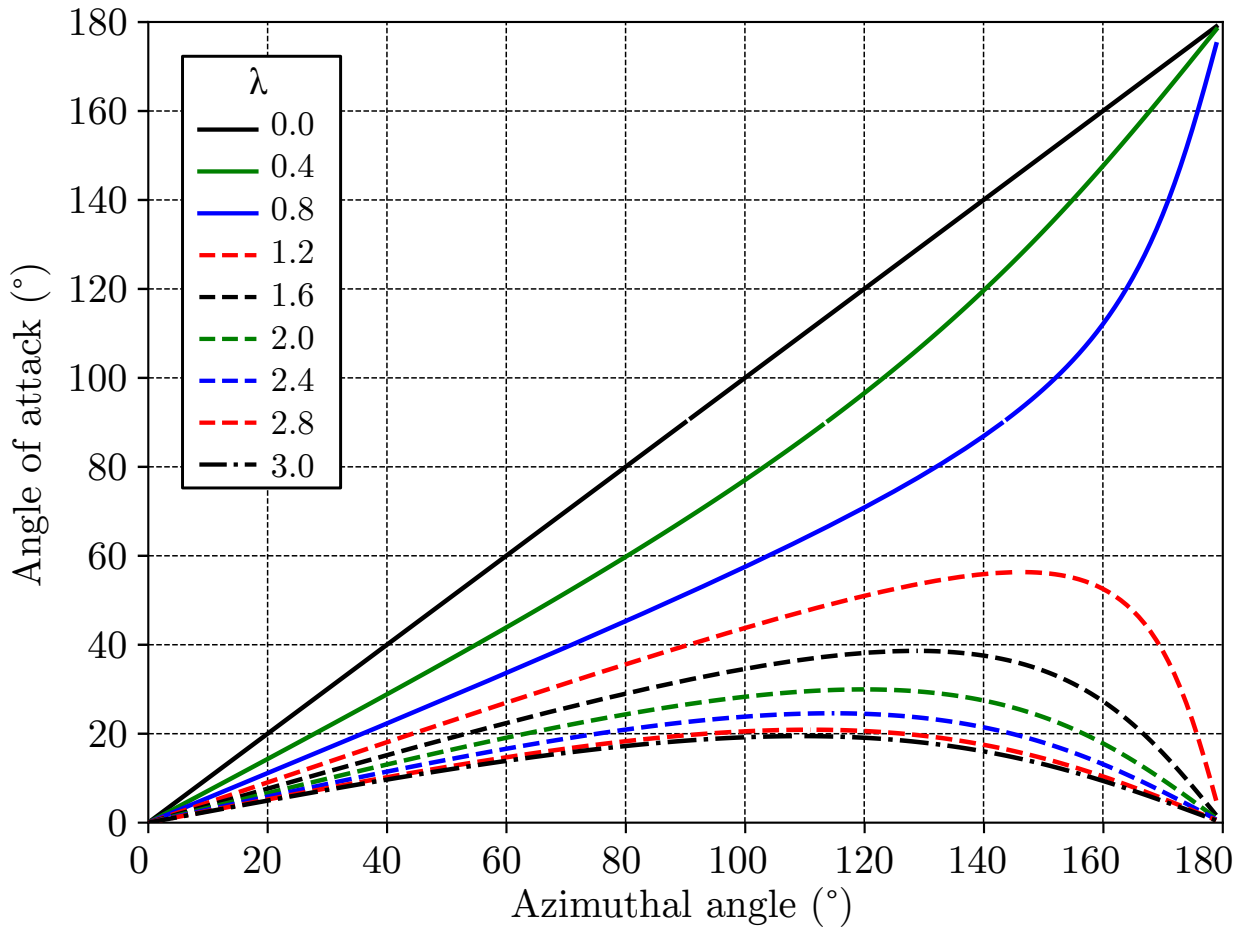
This is the author's peer reviewed, accepted manuscript. However, the online version of record will be different from this version once it has been copyedited and typeset.

PLEASE CITE THIS ARTICLE AS DOI: 10.1063/1.50045083



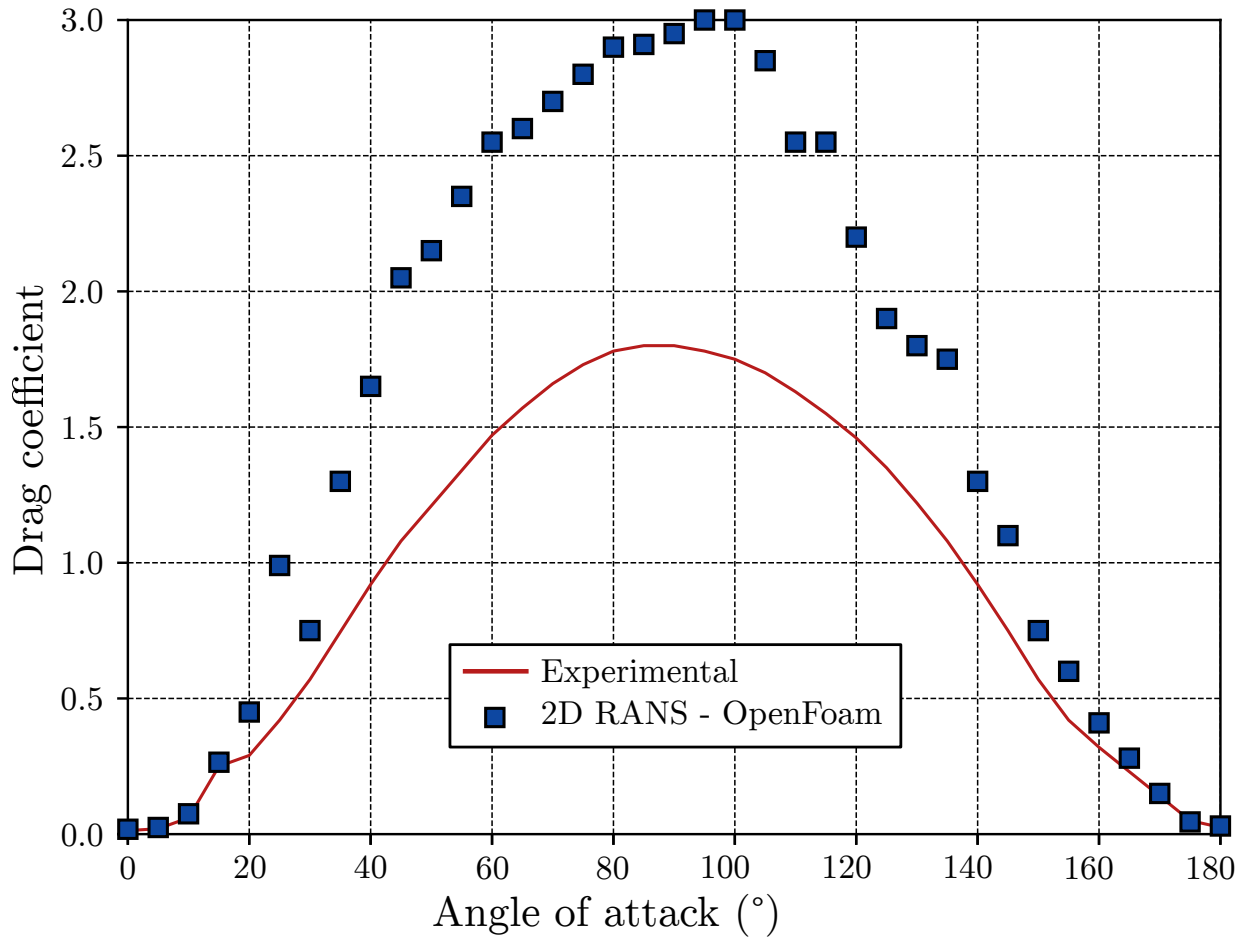
This is the author's peer reviewed, accepted manuscript. However, the online version of record will be different from this version once it has been copyedited and typeset.

PLEASE CITE THIS ARTICLE AS DOI: 10.1063/1.50045083



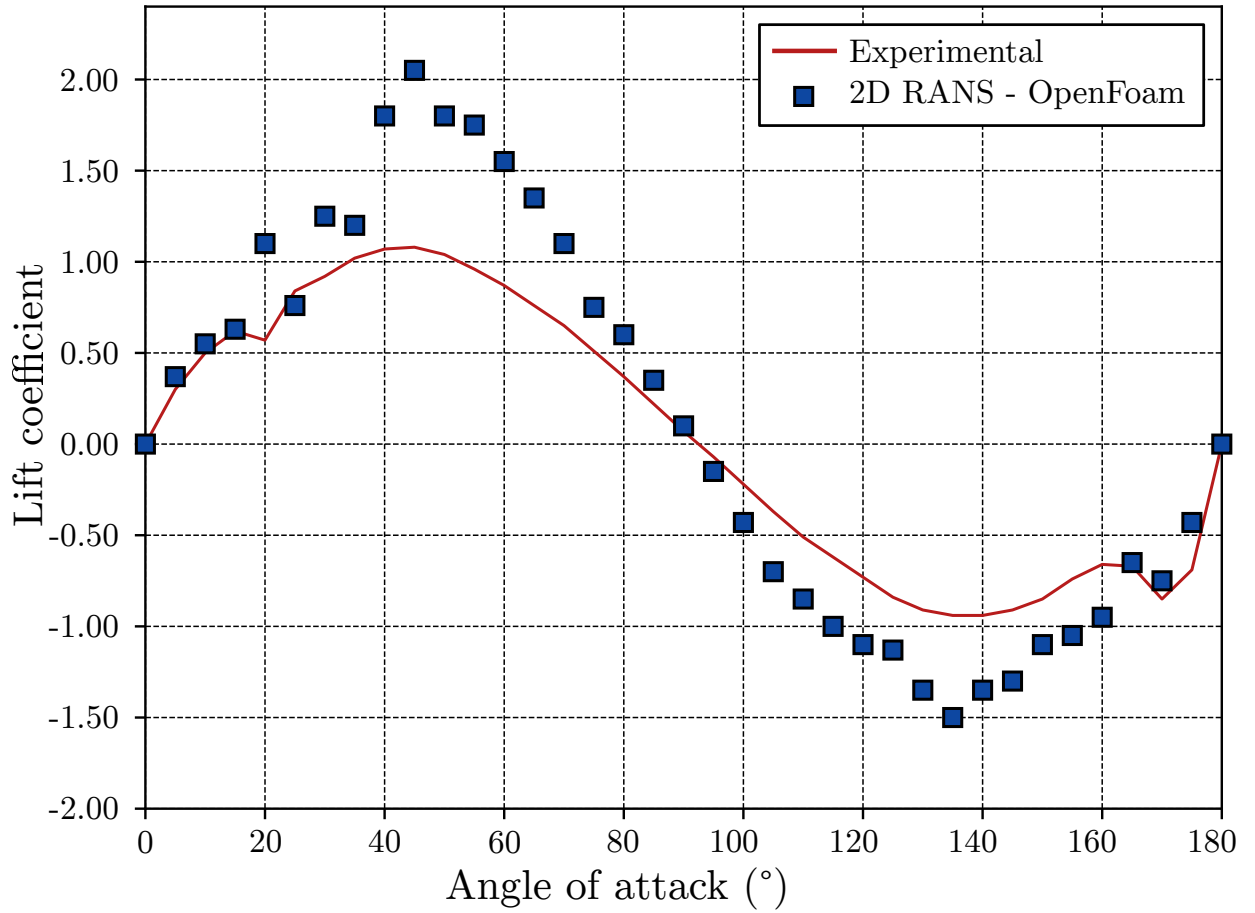
This is the author's peer reviewed, accepted manuscript. However, the online version of record will be different from this version once it has been copyedited and typeset.

PLEASE CITE THIS ARTICLE AS DOI: 10.1063/5.0045083



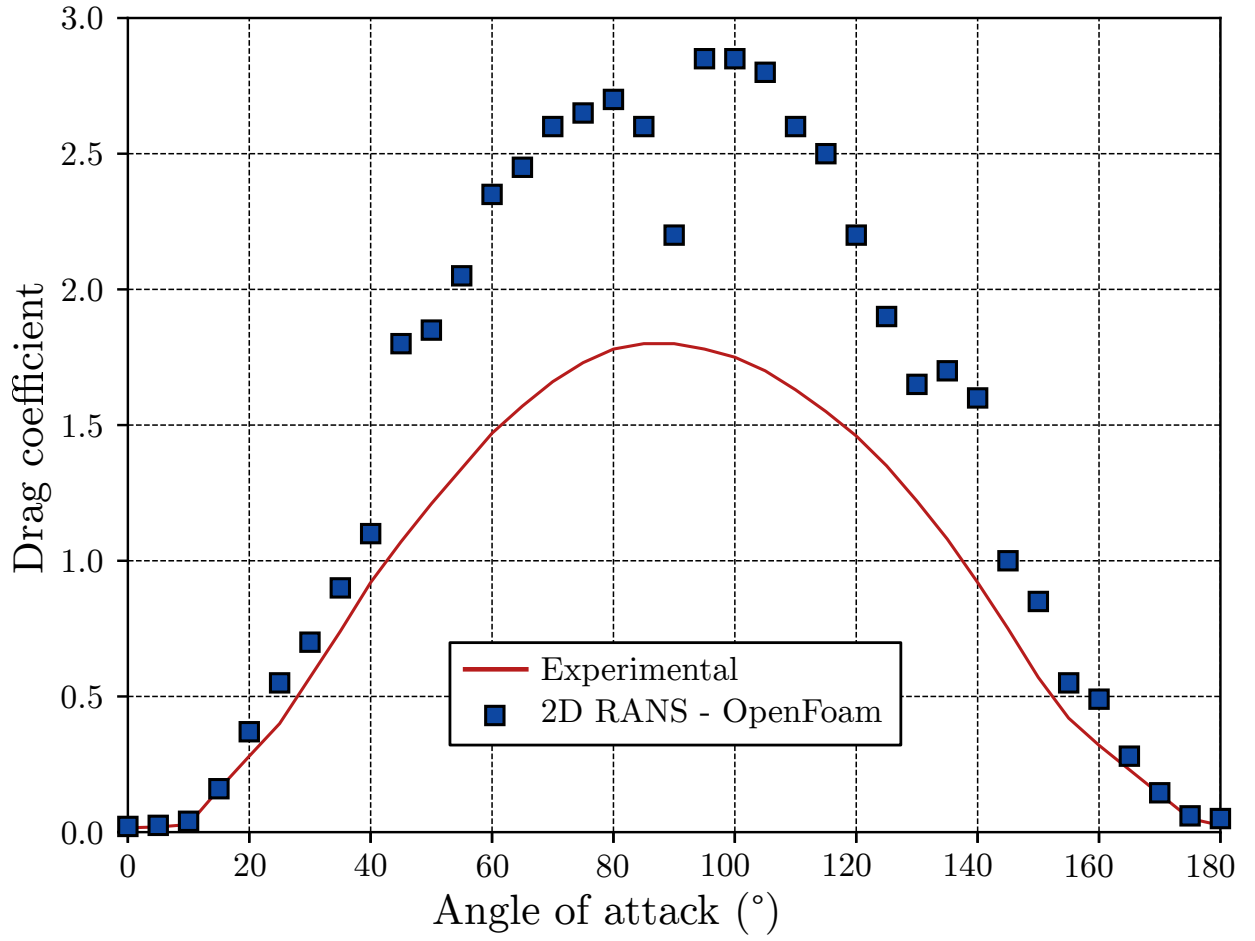
This is the author's peer reviewed, accepted manuscript. However, the online version of record will be different from this version once it has been copyedited and typeset.

PLEASE CITE THIS ARTICLE AS DOI: 10.1063/5.0045083



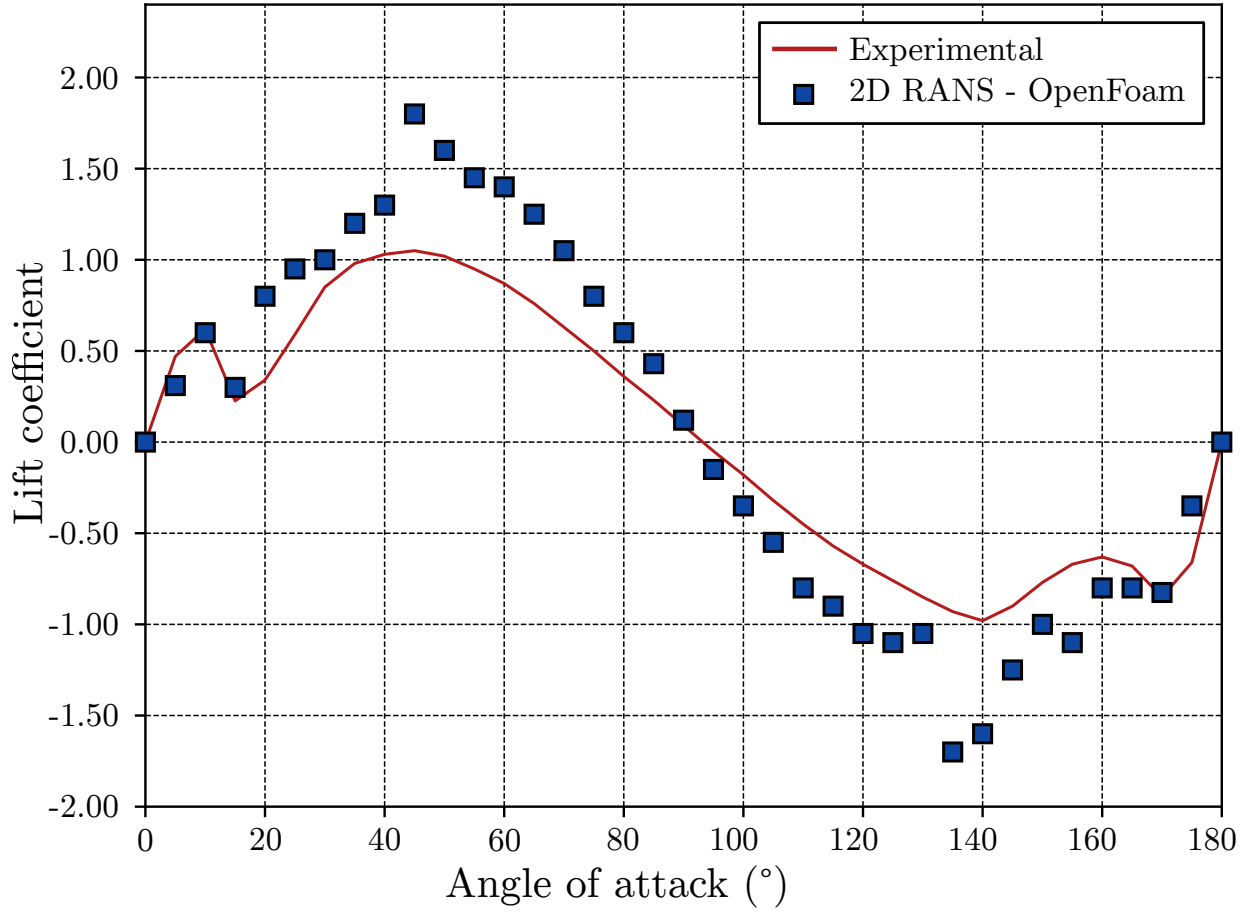
This is the author's peer reviewed, accepted manuscript. However, the online version of record will be different from this version once it has been copyedited and typeset.

PLEASE CITE THIS ARTICLE AS DOI: 10.1063/5.0045083



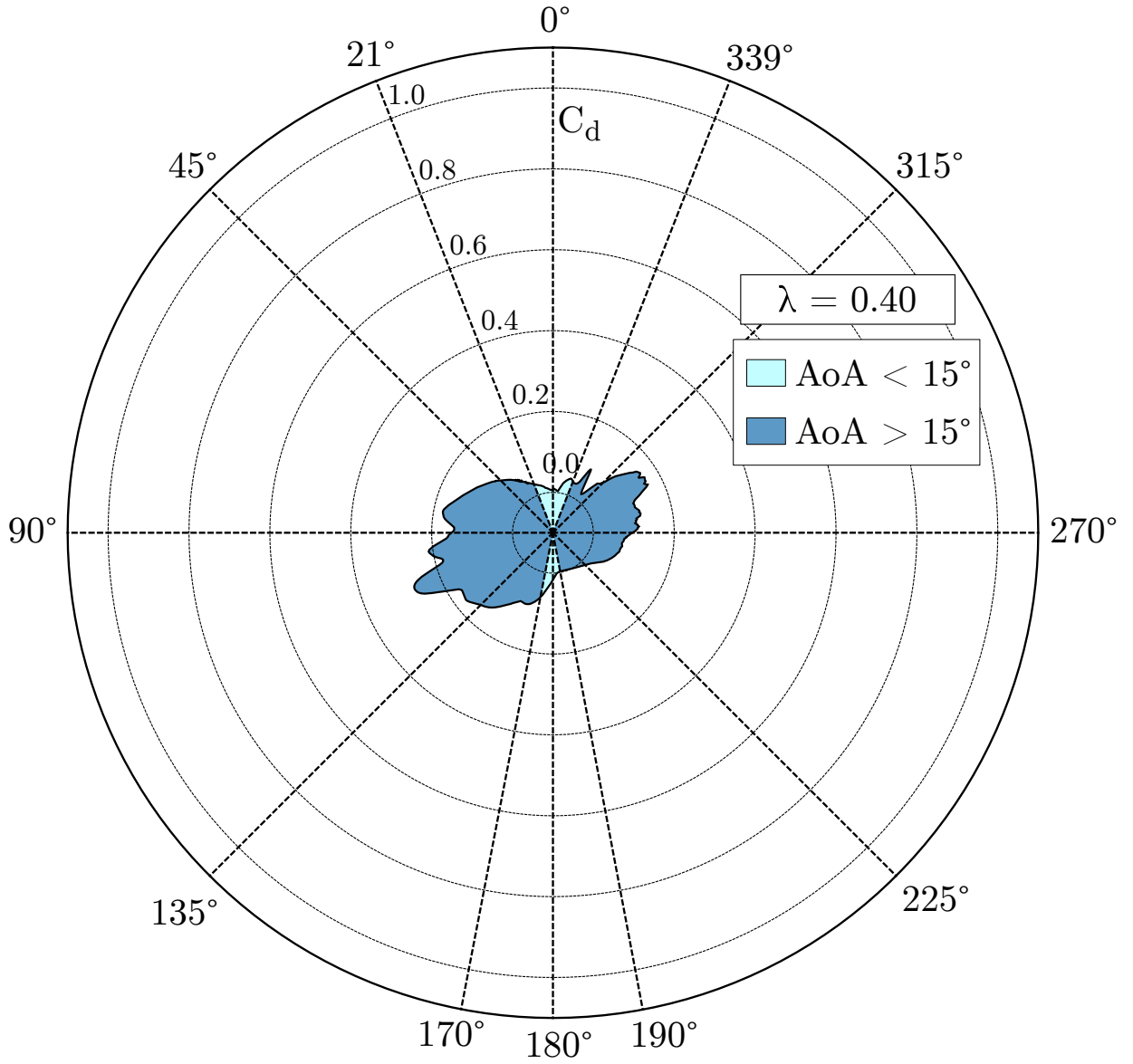
This is the author's peer reviewed, accepted manuscript. However, the online version of record will be different from this version once it has been copyedited and typeset.

PLEASE CITE THIS ARTICLE AS DOI: 10.1063/5.0045083



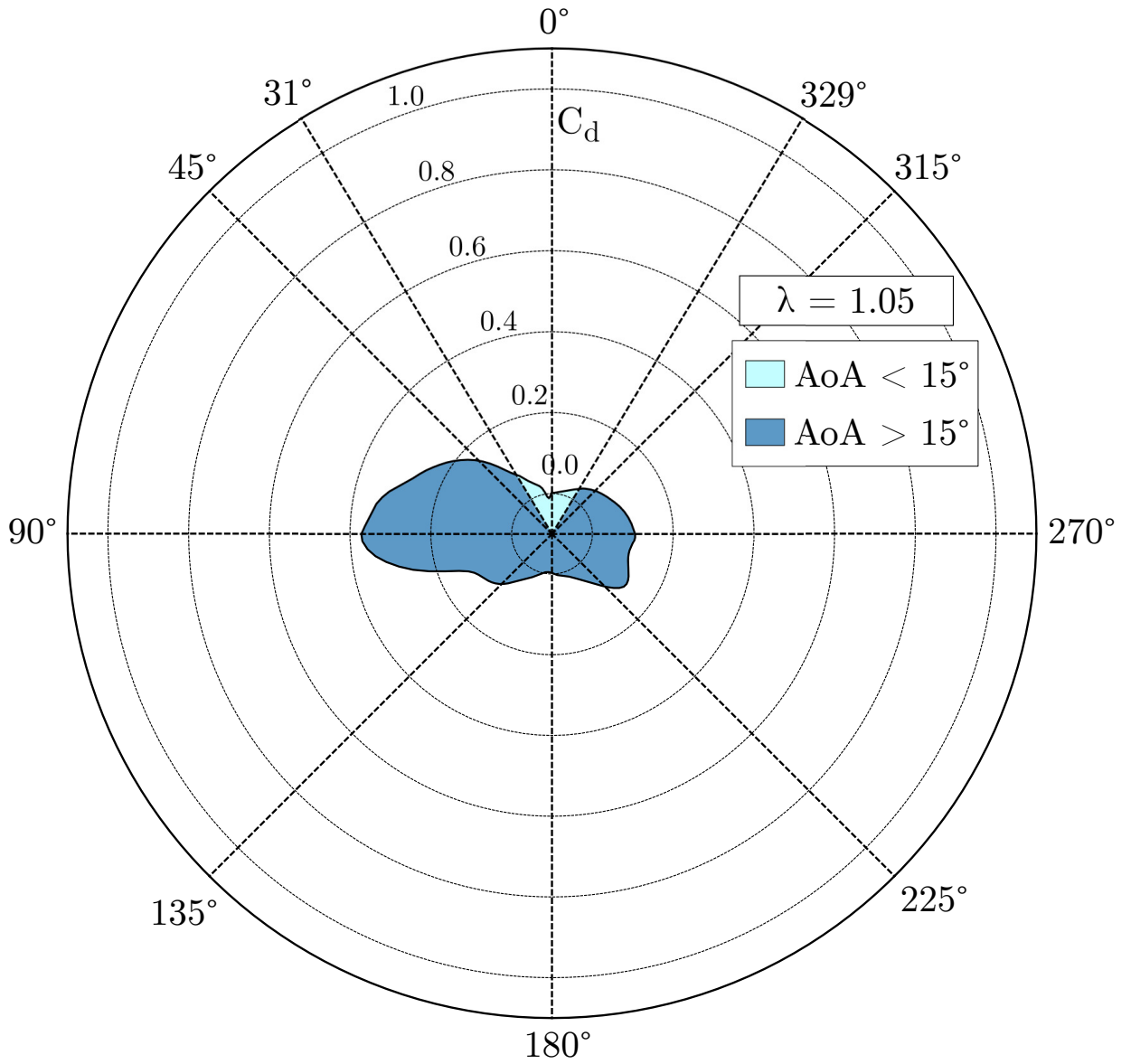
This is the author's peer reviewed, accepted manuscript. However, the online version of record will be different from this version once it has been copyedited and typeset.

PLEASE CITE THIS ARTICLE AS DOI: 10.1063/1.50045083



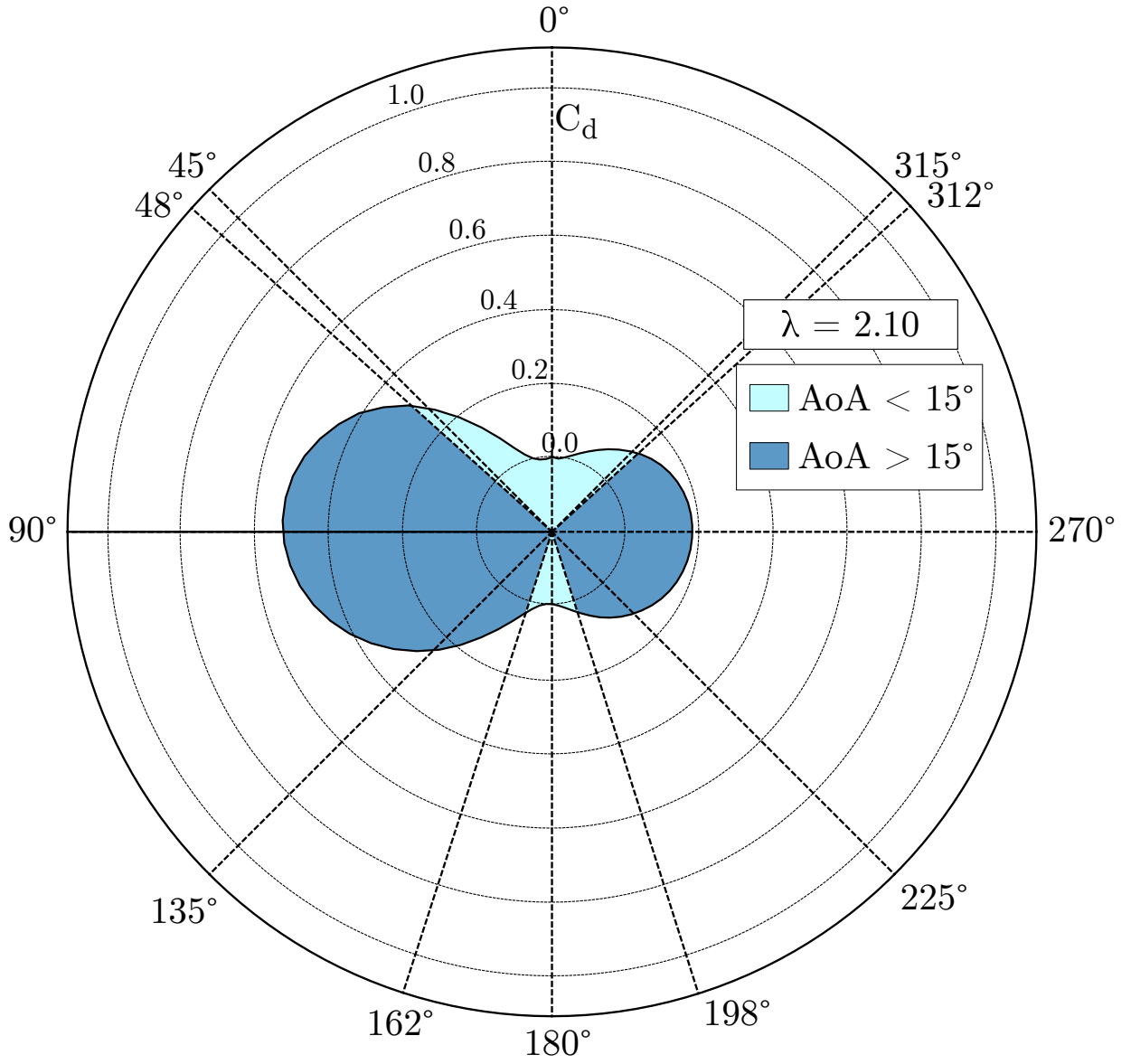
This is the author's peer reviewed, accepted manuscript. However, the online version of record will be different from this version once it has been copyedited and typeset.

PLEASE CITE THIS ARTICLE AS DOI: 10.1063/5.0045083



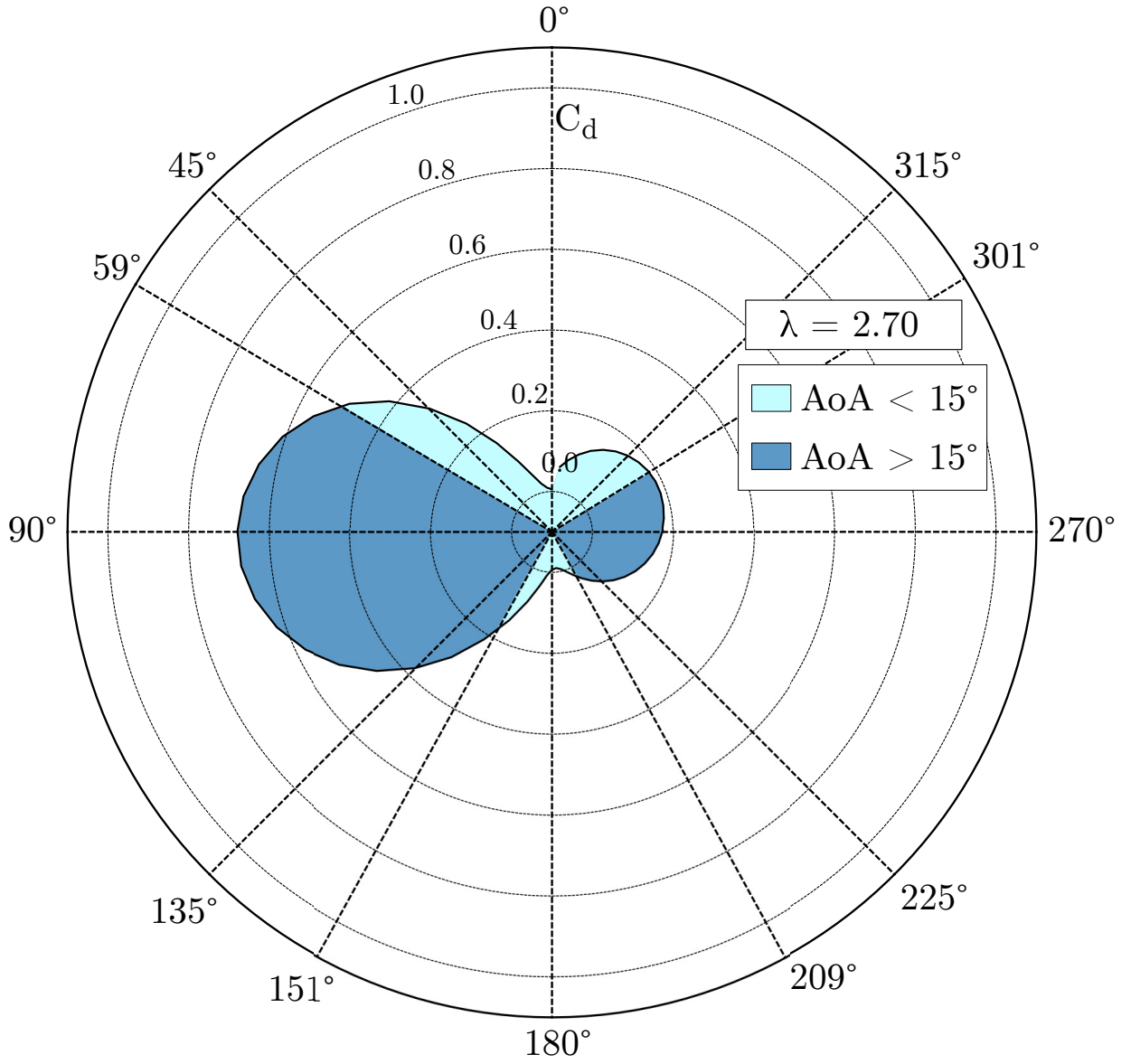
This is the author's peer reviewed, accepted manuscript. However, the online version of record will be different from this version once it has been copyedited and typeset.

PLEASE CITE THIS ARTICLE AS DOI: 10.1063/5.0045083



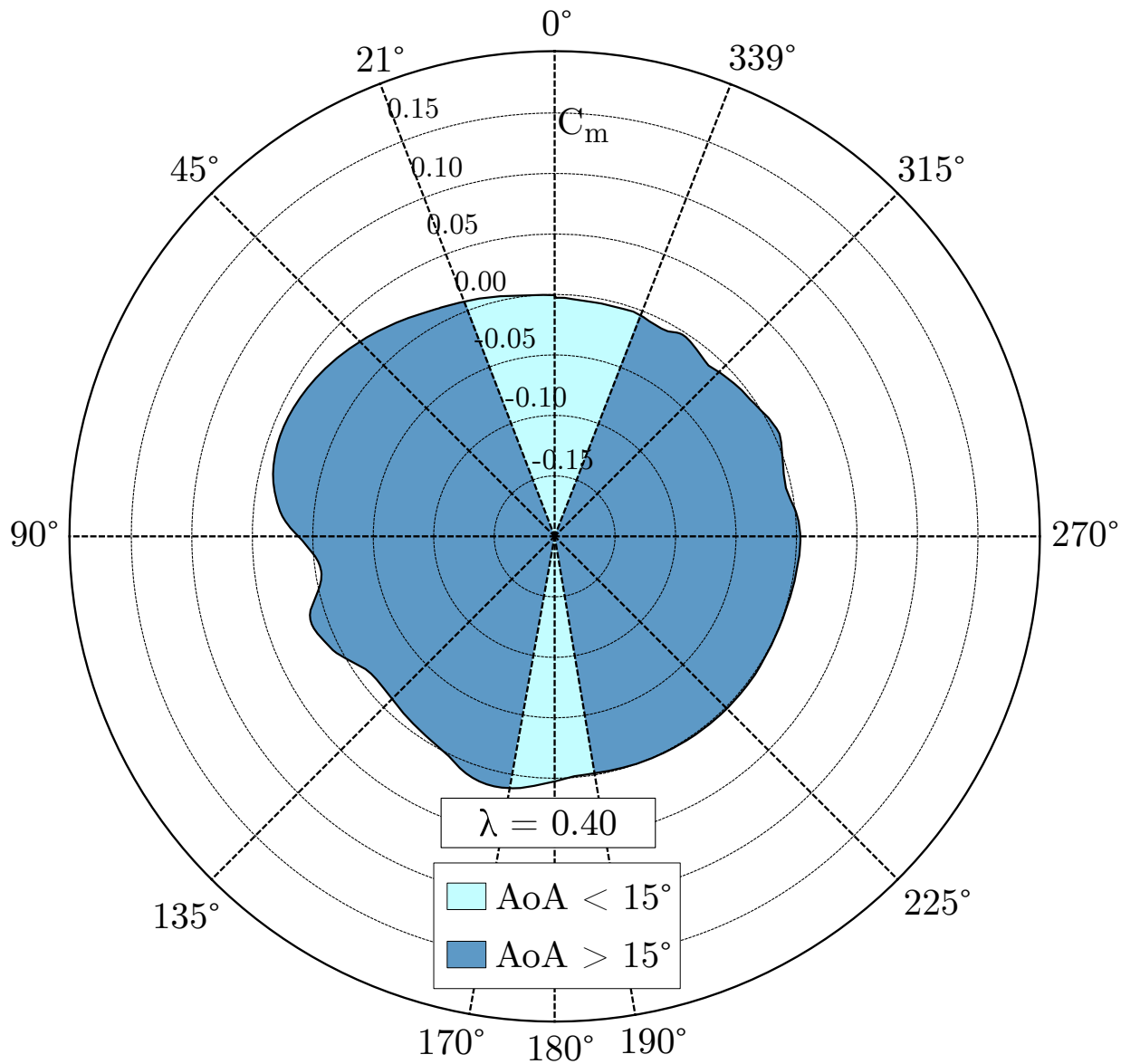
This is the author's peer reviewed, accepted manuscript. However, the online version of record will be different from this version once it has been copyedited and typeset.

PLEASE CITE THIS ARTICLE AS DOI: 10.1063/5.0045083



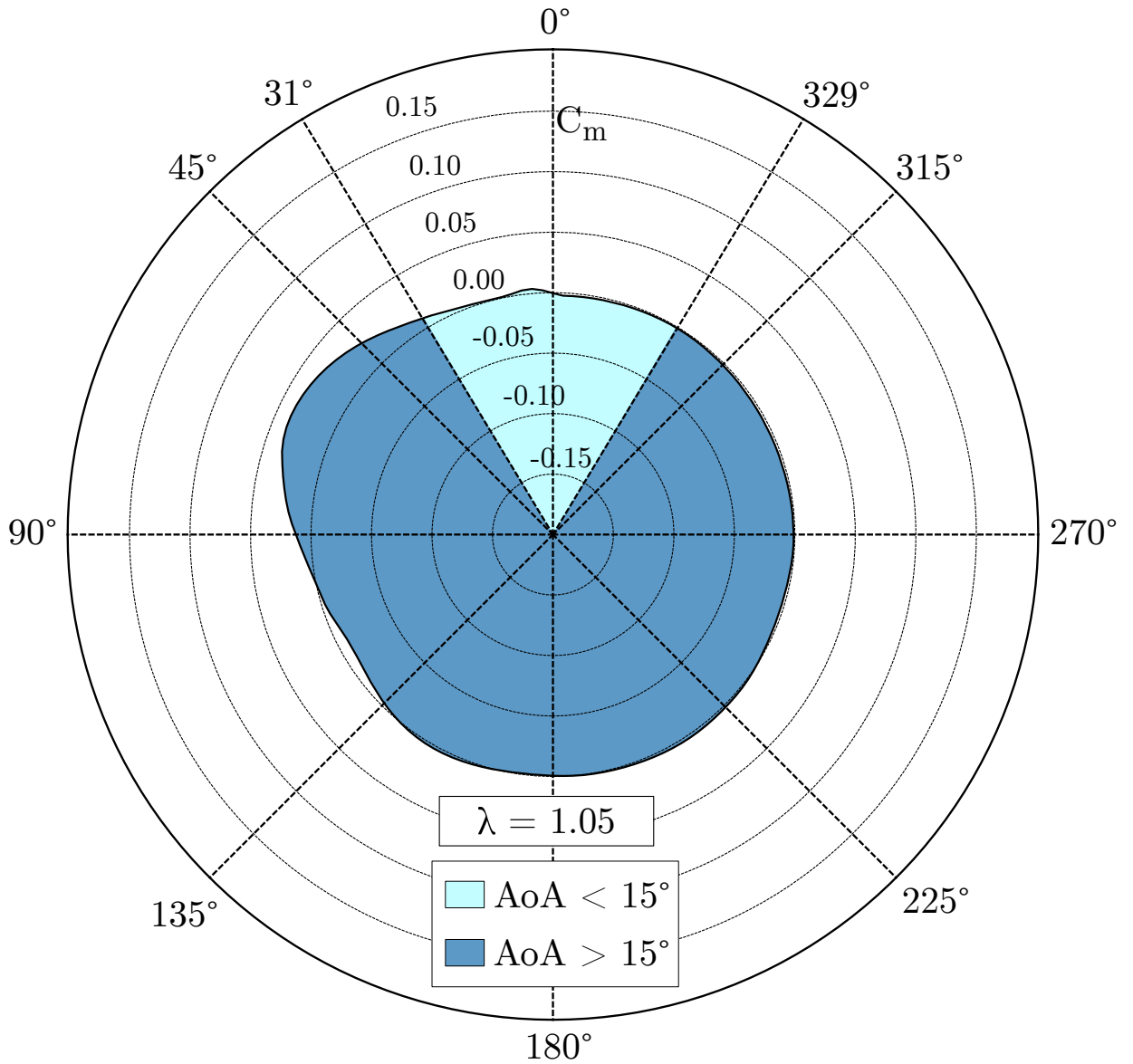
This is the author's peer reviewed, accepted manuscript. However, the online version of record will be different from this version once it has been copyedited and typeset.

PLEASE CITE THIS ARTICLE AS DOI: 10.1063/5.0045083



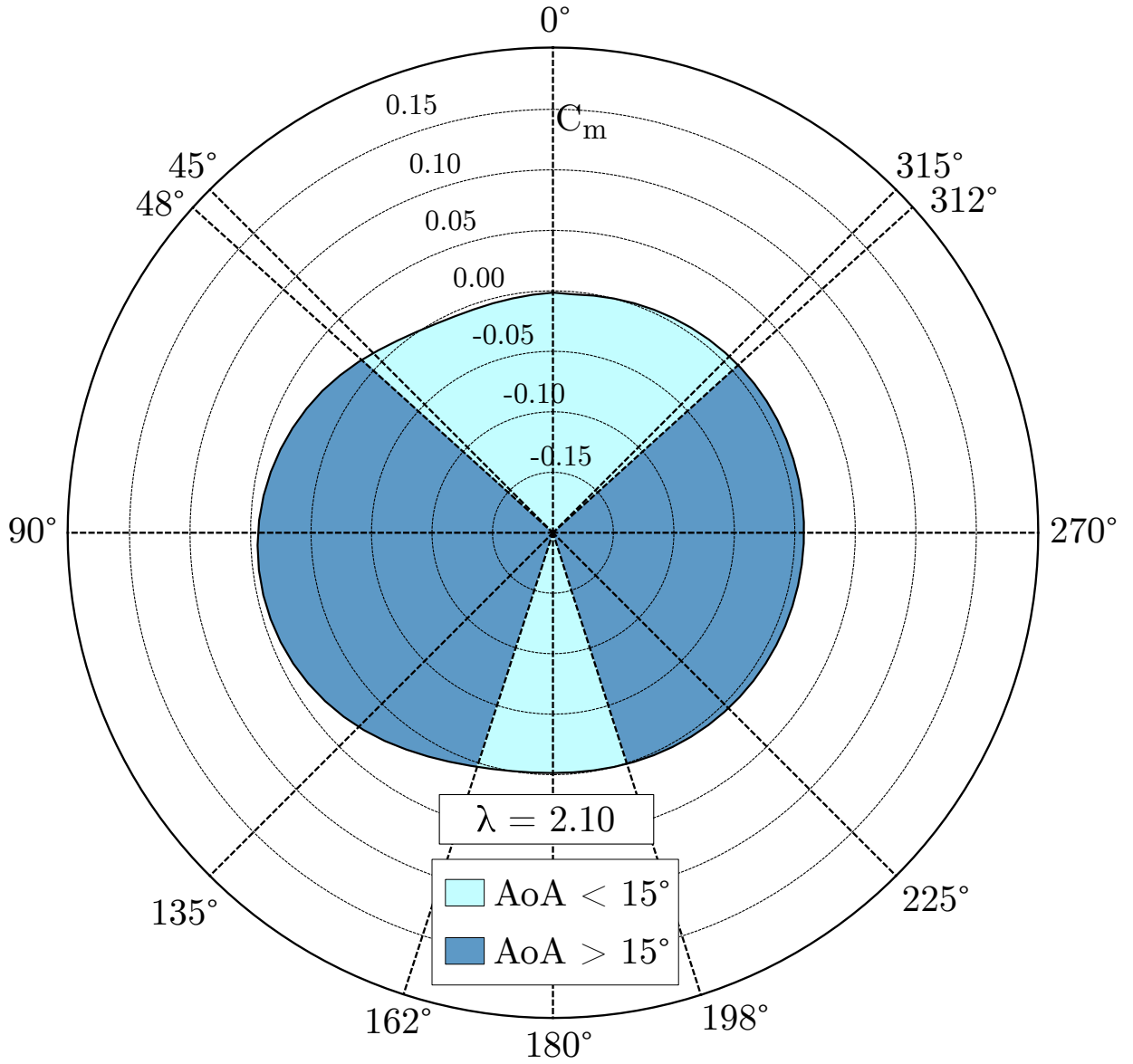
This is the author's peer reviewed, accepted manuscript. However, the online version of record will be different from this version once it has been copyedited and typeset.

PLEASE CITE THIS ARTICLE AS DOI: 10.1063/5.0045083



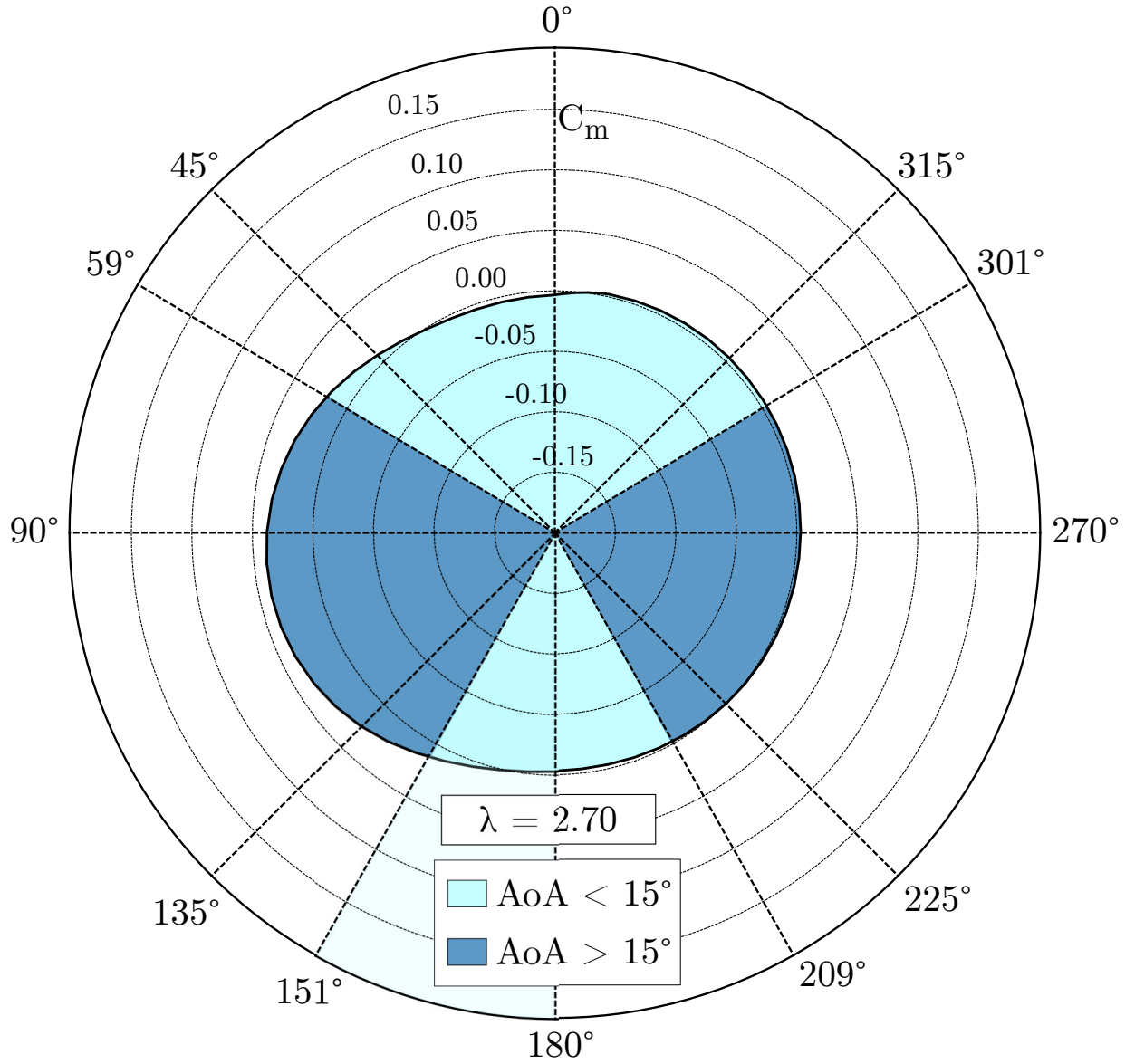
This is the author's peer reviewed, accepted manuscript. However, the online version of record will be different from this version once it has been copyedited and typeset.

PLEASE CITE THIS ARTICLE AS DOI: 10.1063/5.0045083



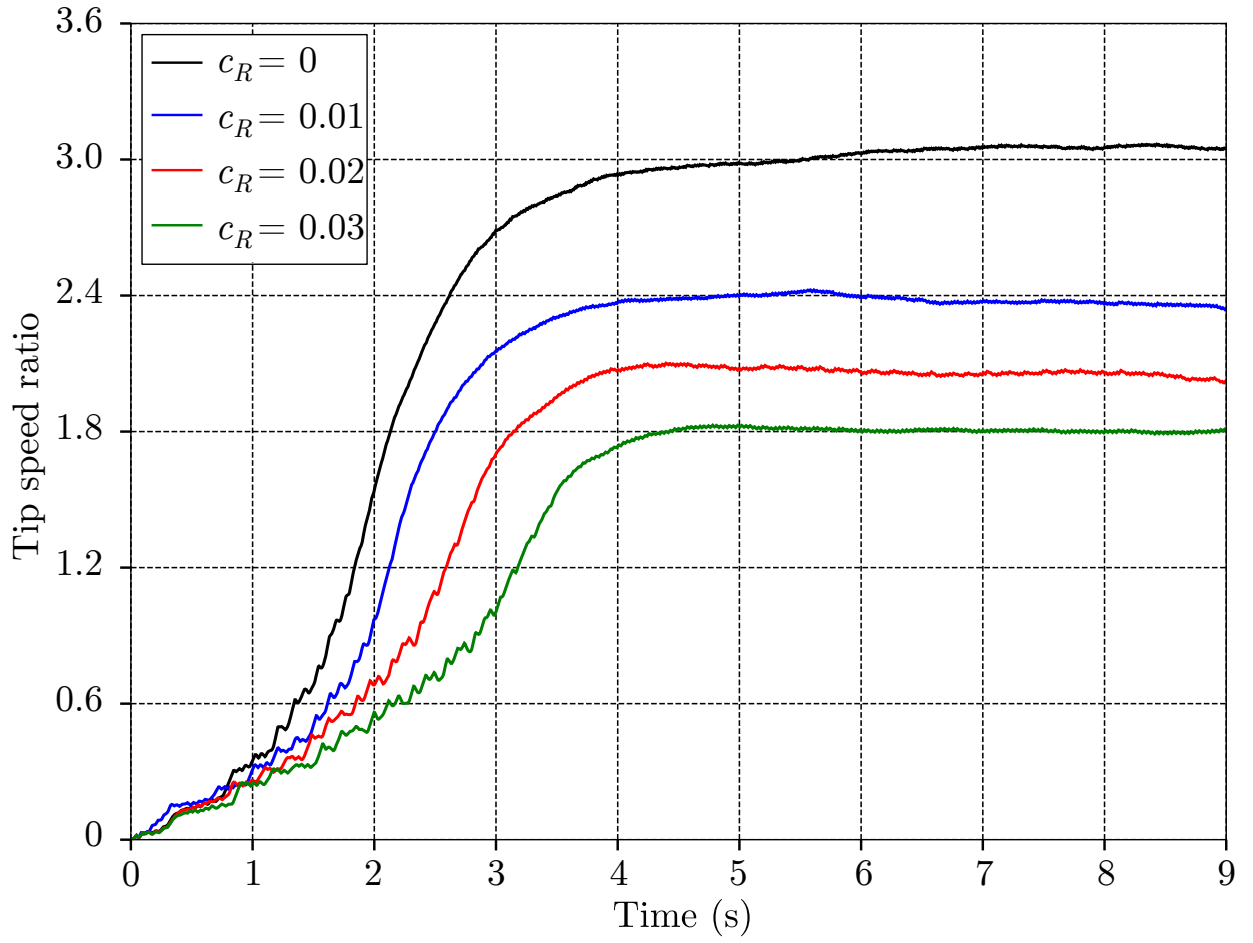
This is the author's peer reviewed, accepted manuscript. However, the online version of record will be different from this version once it has been copyedited and typeset.

PLEASE CITE THIS ARTICLE AS DOI: 10.1063/5.0045083



This is the author's peer reviewed, accepted manuscript. However, the online version of record will be different from this version once it has been copyedited and typeset.

PLEASE CITE THIS ARTICLE AS DOI: 10.1063/1.50045083



This is the author's peer reviewed, accepted manuscript. However, the online version of record will be different from this version once it has been copyedited and typeset.

PLEASE CITE THIS ARTICLE AS DOI: 10.1063/1.50045083

